microwave JOURNAL

contents

VOLUME 25, NUMBER 7
USPS 396-250
JULY 1982

ON THE COVER: Aydin Microwave's new flatpack amplifiers can save valuable space in low noise and limiting amplifier applications. See the Cover Story on p. 108.

*Euro-Global Edition Only.

Press run for this issue is 44,985 copies.

EXECUTIVE EDITORIAL OFFICE
610 Washington Street, Dedham, MA 02026
Tel: 617 326-8220 710 348-0481
TELEX: 951-659
MICROSOL DEDM

EUROPEAN EDITORIAL OFFICE
25 Victoria Street London SW1H OEH England
Tel: 01-222-0466 **TELEX:** 885744

Microwave Journal is issued without charge upon written request to qualified persons working in that portion of the electronics industry including governmental and university installation that deal with VHF through light frequencies. Other subscriptions; domestic, $36 per year, two year subscriptions $65; foreign, $48 per year, two year subscriptions $85: back issues (if available) and single copies $5.00.

POSTMASTER: send address corrections to Microwave Journal, 610 Washington Street, Dedham MA 02026.

BPA

Horizon House also publishes Telecommunications and Journal of Electronic Defense

A Coherent, Solid State, 225 GHz Receiver

Ronald E. Forsythe
Georgia Institute of Technology
Atlanta, GA

Introduction

The receiver is a critical element in the development of high performance systems in the upper regions of the millimeter wave frequency range (140-340 GHz). Some improvement in system performance can be obtained due to reduced aperture size and/or antenna resolution by going to these high frequencies. However,the presence of higher atmospheric losses tends to degrade system performance at a rate that nearly offsets the improvement obtained due to increased resolution. These losses reduce the amount of available signal level in both passive and active systems. In addition, high transmitter power becomes more difficult to obtain, especially with solid state sources at these frequencies. For these reasons low noise receiver performance remains an item of high priority in most systems.

Recently reported developments in the area of receiver technology in this frequency range show some remarkable improvements in receiver sensitivity [1-4]. However, system applicability is still the key in any receiver design. Such criteria as bandwidth, size, power requirements, dynamic range, noise figure, and reliability are examples of some of the parameters that are considered when choosing a particular technique for downconverting energy in any receiver.

As the development of fieldable systems continues into this region of the millimeter wave frequency range, the problem of obtaining clean, low cost, solid state, phase locked local oscillators continues to exist. A new low noise, broadband, balanced mixer that alleviates this problem has recently been developed at Georgia Tech for use as a 225 GHz receiver [5,6]. It uses a local oscillator (LO), whose frequency is nearly one fourth the signal frequency, to mix the signal power to a low IF, which is then amplified. This same LO drives a similar mixer that is used to phase lock a 225 GHz transmitter.

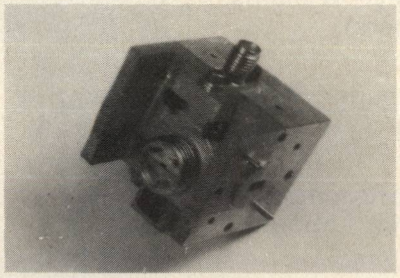

Fig. 1 A 225 GHz fourth subharmonic mixer.

Other options were considered as receiver candidates including a fundamental mixer and a subharmonic mixer using a LO at about one half the signal frequency. Both of these require considerable effort to obtain a low noise, phase locked local oscillator that could drive two mixers simultaneously, A 112.5 or 225 GHz local oscillator with sufficient power could possibly be obtained using a multiplifer and a Klystron tube source, but the power needed to drive both mixers using all solid state sources would be very difficult, if not impossible, to obtain with today's technology. The fundamental mixer has additional problems associated with the development of a low loss RF/LO coupling network.

Mixer Description

This mixer, shown in Figure 1, was designed using a low frequency (6.86 GHz) model and scaled up in frequency (down in size) using a scaling factor of 32. It uses a combination of suspended substrate stripline circuits with two low pass filters, two waveguides (LO and RF), and a pair of antiparallel diodes to achieve the low loss conversion characteristics needed for this receiver. It has been designed to be scalable up to 340 GHz. The diode contacting wire size, diode chip size, and diode junction capacitance were considered, as well as the circuit and waveguide dimensions, during the development of the low frequency scaled model.

The antiparallel diode pair circuit is shown in Figure 2. This particluar arrangement of diodes has the properties of suppressing all even numbered mixing products, such as those occuring at $|F_s \pm F_{LO}|$, $|F_s \pm 3F_{LO}|$, and the dc or video component without the aid of any external filters or circuits. These frequencies all appear

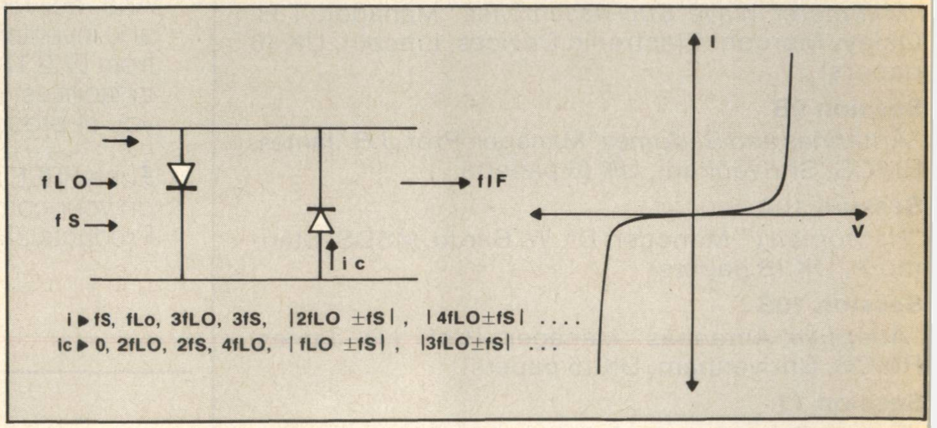

Fig. 2 Antiparallel diode circuit.

[Continued on page 66]

aves Conference

Session 4A
"IR Components and Sub-Assemblies" Manager: R.C. Parry, MEL, Crawley, UK (4 papers)

Session 4B
"Microwaves in Remotely Piloted Vehicles and Guided Weapons" Manager: D.M. Clunie, MoD (Pe), London, UK (4 papers)

Session 5A
"Optical Processing" Manager: P.D.L. Williams, Racal-Decca, Chessington, UK (5 papers)

Session 5B
"Transmitters and Components" Manager: Dr. J. Clarke, RSRE, Malvern, UK (6 papers)

Session 6A
"Broadband Components and Sub-Assemblies" Manager: L.W. Chua, Philips Research Laboratories, Redhill, UK (5 papers)

Session 6B
"Applications of High Speed Digital Processing" Manager: Dr. J.R. Forrest, University College, London (5 papers)

Session 7A
"Passive EW" Manager: M. Thurbon, System Designers Ltd., Fleet, UK (5 papers)

Session 7B
"Navigation" Manager: P.K. Blair, Standard Telecommunications Laboratories, Harlow, UK (4 papers)

Session 8A
"Active EW" Manager: B.P. Blaydes, MoD (Pe), London (4 papers)

Session 8B
"Instrumentation" Manager: B. Jackson, Thorn-EMI, Wells, UK (4 papers)

Session 9A
"Millimeter Wave Sub-Assemblies" Manager: T.H. Oxley, Marconi Electronic Devices, Lincoln, UK (6 papers)

Session 9B
"Antennas and Radomes" Manager: Prof. J.R. James, RMCS, Shrivenham, UK (6 papers)

Session 10A
"Radiometry" Manager: Dr. W. Bardo, MSDS, Stanmore, UK (5 papers)

Session 10B
"Adaptive Antennas" Manager: Prof. J.R. James, RMCS, Shrivenham, UK (5 papers)

Session 11
"Future Prospects for 1 GHz to 1 μm" Manager: Dr. J.R. Forrest, University College, London (3 papers)

in the circulating current (I_c) where they are, hopefully, reactively terminated or suppressed. The total current (I) contains the frequencies of interest for subharmonic mixing such as $|F_s \pm 2F_{LO}|$ and $|F_s \pm 4F_{LO}|$[7, 8]. The latter mixing product is of partucular interest in this case, and represents the IF frequency component for subharmonic mixing using the fourth harmonic of the LO that is developed in the diode pair. To obtain lower loss conversion to this mixing product, an external circuit is needed to suppress the second harmonic mixing product.

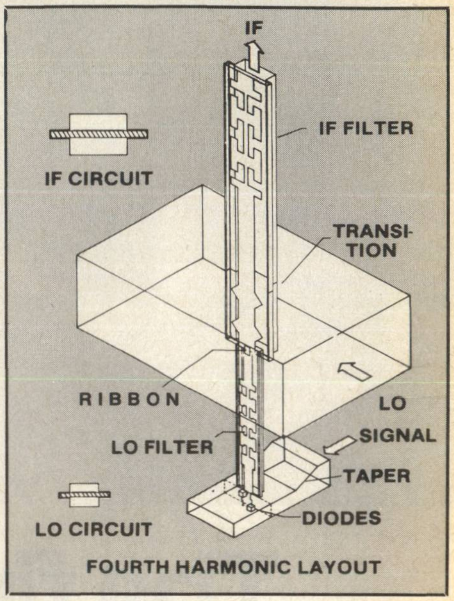

Fig. 3 Functional diagram of fourth subharmonic mixer.

This mixer, shown diagramatically in Figure 3, uses WR-5 waveguide for the signal input and WR-19 waveguide for the LO input. Both waveguides have tunable backshorts for matching the LO and RF energy to the diodes. The diodes are mounted in the reduced height signal waveguide so that they are antiparallel to the E-field as shown in Figure 4. The diodes are GaAs diode chips with an array of 1.5 μm Schottky diodes formed on the face perpendicular to the two NiAu wires which make the contact to the diodes. The wires are 0.0005" in diameter. They are formed into small springs and the tips are chemically etched to a fine point. A diode chip and a wire are each mounted on separate pins that are press fit into the portion of the mixer body that forms

[*Continued on page 68*]

[From page 66] **RECEIVER**

the bottom wall of the signal waveguide. Another diode chip and wire are soldered into place on the center conductor of the substrate circuit at the top of the signal waveguide wall. The pins are then slowly pressed in one at a time until each diode is contacted. This entire process is done in an open structure so that the diodes and whiskers can be closely monitored under a microscope.

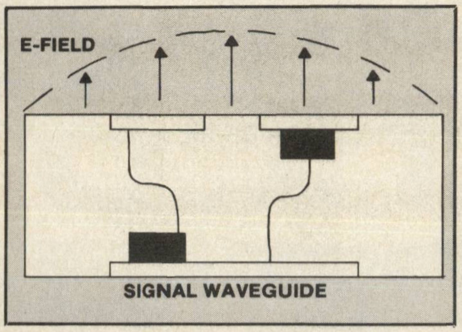

Fig. 4 Diode and contacting wire arrangement in signal waveguide.

The suspended substrate stripline circuits, shown in Figure 5, perform several functions as outlined in Table 1. The smaller filter (LO filter) is a low impedance high impedance, nine element, low pass filter. It helps match the RF energy to the diodes and keeps the RF energy in the signal waveguide. It also passes the LO frequency to the diodes, passes the IF frequency to the larger circuit, and helps suppress the generation of the second harmonic mixing product by providing a reactive termination at twice the LO frequency. The larger filter (IF filter) is a seven element low pass filter. The lower part of its center conductor is located in the middle of the LO waveguide, parallel to the E-field. This filter acts as a waveguide to stripline transition and a LO/IF diplexer, reflecting

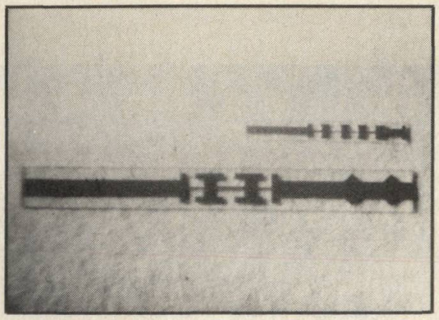

Fig. 5 Photomicropraph of quartz suspended substrate stripline circuits.

the LO energy from the low pass filter, in order to provide maximum coupling of the LO to the diodes. The cutoff frequency of this filter is chosen so that it passes the IF frequency to an external SMA connector with low loss. A gold ribbon is soldered to the center conductors of the two circuits to connect them. A larger circuit can be used for the upper filter functions because only the lower frequencies are present, and higher order modes are not a problem. Better filter performance could be obtained using this larger circuit because higher impedance ratios could be more easily realized. These filters are broadband and were easily scaled because they do not require the tolerances needed for accurate scaling of typical band pass filters. The smallest dimensions of the lines are on the order of 0.001 to 0.002 inches, which are easily obtainable with common photolithographic techniques. The center conductors are a Cr-Au metalization which has been vacuum deposited on 0.0025 or 0.005 inch thick quartz substrates.

TABLE 1
225 GHz RECEIVER NOISE FIGURE SUMMARY

Item	Measured
Horn/Transition Loss*	1.5 dB
Mixer Noise Figure (DSB)	8.5 dB
IF Preamp Noise Figure	2.0 dB
Total Noise Figure	120. dB

*Estimated

Receiver Description

The receiver, shown in Figure 6, consists of a conical corrugated horn antenna, a subharmonically pumped mixer, a 56 GHz phase locked Gunn oscillator, a variable attenuator and a 500-1000 MHz IF preamplifier. The horn contains a circular to rectangular (WR-4) waveguide transistion and a WR-4 to WR-5 waveguide transistion. It is electroformed and is used to feed the quasi-optical components (lenses, diplexers, ect.). that are part of the system's front end. A summary of receiver performance is given in Table 2.

The 56 GHz Gunn oscillator is a

[Continued on page 70

[From page 68] **RECEIVER**

commercially available phase locked source with 50 mW output. This device is used to operate both a phase lock mixer (used to phase lock the transmitter) and the receiver mixer. A waveguide three dB coupler is used to divide the power to drive the two mixers simultaneously.

Mixer Performance

The mixer built at 225 GHz was measured to have an 8.5 db DSB noise figure using a standard Y factor measurement over a 500-1000 MHz IF. This compares well with the 5 dB noise figure predicted by the model. The device was measured with higher IF's to determine its instantaneous bandwidth capabilities. A noise figure degradation of only 0.5 to 1.0 dB was measured over a 2-4 GHz IF bandwidth, and the 3 dB bandwidth was measured to be greater than 10 GHz. This measured bandwidth also compares well with that predicted by the model mixer.

These devices have been ruggedized for both ground based field use and airborne measurement programs (both low and high altitude). Similarly built devices have been used on a P-3 aircraft and B-57 aircrafts taking passive millimeter wave imaging data at 220 and 183 GHz, respectively.[9,10]

TABLE II. FILTER PARAMETERS AND DATA

Filter	Scaled f_{cs}	Actual f_c	Insertion Loss $IL_{Sig.}$	IL_{LO}	IL_{2XLO}	IL_{IF}
IF	0.9 GHz	29 GHz	—	39dB	—	0.1 dB
LO	2.8 GHz	90 GHz	50dB	0.1dB	30dB	0.1dB

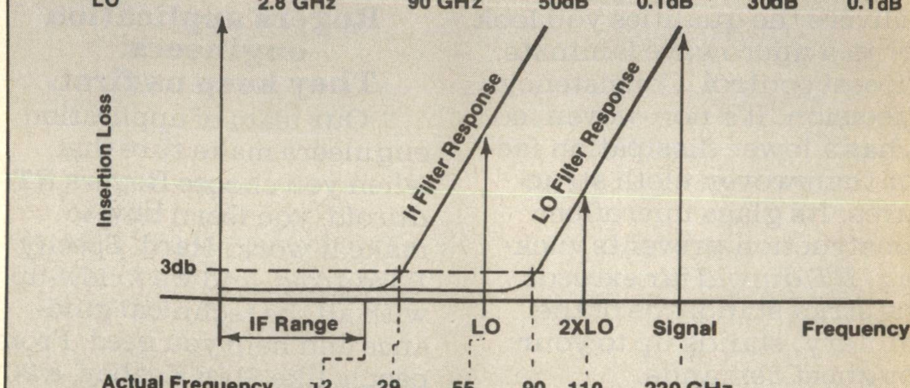

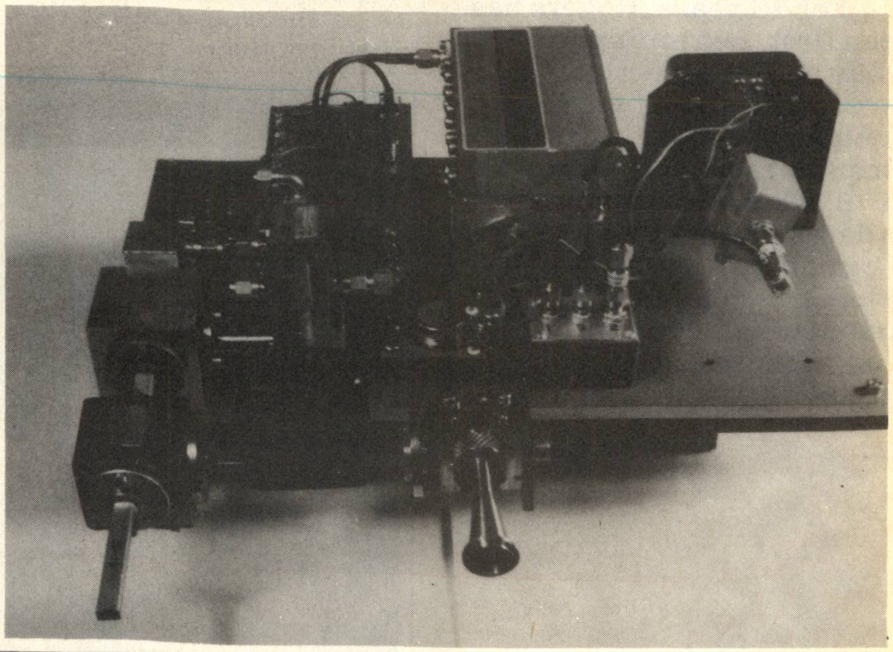

Fig. 6 The 225 GHz coherent receiver.

The total receiver noise figure of 12 dB (DSB) could easily be lowered to about 10 to 10.5 dB by using a lower noise IF preamplifier and a lower loss horn. Better mixer noise figures should also be possible because these are only the first mixers of this kind to be built. A mixer noise figure of 7.0 dB should be achievable with these devices.

Summary

The development of mixers that use a local oscillator at one fourth the signal frequency and can still provide broadband, low noise performance characteristics is a substantial breakthrough in millimeter wave receiver technology. The use of subharmonic mixers lowers LO cost, noise, and complexity, increases LO availability and reliability, and is compact and portable. For instance, the current 225 GHz version of this receiver can fit in a 3″ x 3″ x 3″ package when driven by a simple free running Gunn LO. The use of such a low LO frequency also increases the options available for developing fully integrated circuit receivers, especially at 90 and 140 GHz.

The bandwidth of this receiver is currently limited by the 500-100 MHz IF preamplifier. This bandwidth could easily be increased to 10 GHz using a stepped LO approach and a broader band IF amplifier. The 10 GHz limitation is currently caused by the nature of the LO filter. This conclusion is based on measurements made with the low frequency model. Versions of the mixer with even broader bandwidths are possible because there are no frequency limiting circuits prior to the mixer other than the signal waveguide. Slightly different arrangements of the diodes and stripline circuit could result in full waveguide band operation if properly designed.

Typical applications for these types of mixers include coherent receivers, passive imaging, multiple receiver systems, and broadband detection systems. The most significant development is that low noise, all solid state, compact receivers are now available which can be used in field measurement, systems and airborne applications in the 140-340 GHz frequency range.

Near term efforts in the development of these mixers will be focused on integrating IF preamplifiers, adapting the mixers for use with beam lead diodes, extending the bandwidth capability, reducing noise figure and moving both up and down in frequency to cover the 90, 140, and 340 GHz frequency ranges. Similar mixers using an LO at one half the signal frequency have also been developed and are currently being used in many fielded systems.

Acknowledgments

The diodes used in these devices were provided by R. Mattauch, University of Virginia; G. Wrixon, University of Cork; and G. Hill, Georgia Institute of Technology. Acknowledgment is also given to the following people for their contributions to this effort: D.O. Gallentine (mechanical design); S.M. Halpern and J.A. Shaver (mixer assembly); and J. Lamb NASA/GSFC (circuit fabrication). This work was partially paid for by NASA/GSFC under NASA Grant NSG-5012.

REFERENCES

1. Archer, J., "A Portable, All-Solid-State Low Noise Receiver for 230 GHz, "IEEE Conference on IR and MM Waves, Miami, Florida, December 1981.
2. Erickson, N., "A Cryogenic Receiver for 1 mm Wavelength," IEEE Conference on IR and MM Waves, Miami, Florida, December 1981.
3. Forsythe, R. E., and S. M. Halpern, "Subharmonic Mixers for 183-225 GHz," IEEE Conf. on IR and MM Waves, Miami, Florida, December 1981.
4. Forsythe, R. E., et al., "Development of a 183 GHz Subharmonic Mixer," IEEE-MTT Symposium, May 1979.
5. Forsythe, R. E., "Research in Millimeter Wave Techniques," Semi Annual Reports for NSG-5012, Georgia Institute of Technology, Atlanta, Georgia, January 1979 to January 1982.
6. Forsythe, R. E., "A Coherent 225 GHz Receiver, IEEE Conference on IR and MM Waves, Miami, Florida, December 1981.
7. Cohn, M., et al., "Harmonic Mixing with an Antiparallel Diode Pair," IEEE-MTT, Vol. MTT-8, pp. 667-673, August 1975.
8. Schneider, M. and W. Snell, "Harmonically Pump Stripline Downconverter," IEEE-MTT, Vol. MTT-23, pp. 271-275, March 1975.
9. Hollinger, J. P., et al., "An Airborne Imaging System at 140 and 220 GHz," IEEE Conference on IR and MM Waves, Miami, Florida, December 1981.
10. Gaglino, J. and J. McSheehy, "Airborne Millimeter Wave Radiometer for 94/183 GHz High Altitude Atmospheric Measurements," IEEE Conference on IR and MM Waves, Miami, Florida, December 1981. ■

SAW Devices for Military Communications, Radar, and EW Systems

C.S. Hartmann
R. J. Kansy
RF Monolithics, Inc.
Dallas, TX

W.D. Daniels
B.R. Potter
Texas Instruments, Inc.
Dallas, TX

Introduction

Surface Acoustic Wave (SAW) devices are radio frequency components that exploit the characteristics of a particular class of acoustic waves that propagate on the surface of solids. Electrical coupling to the SAW is directly accomplished on piezoelectric solids. A key feature of the SAW is its accessibility. The wave can be "sampled" at any point along its path. Judicious arrangement and weighting of these samples results in diverse device characteristics.

Most SAW devices to date have been constructed for use in the VHF and UHF bands (30 to 1000 MHz), limited at low frequencies by the size and cost of the substrates and at high frequencies by photolithographic resolution. Applications include monolithic bandpass filters, frequency control components, and signal processing components in which the precise generation of complex waveforms is required.

Saw Fundamentals

—Transversal Filters

The invention of the interdigital transducer was responsible for spurring the development of SAW device technology. The transducer consists of a pattern of interleaved electrodes engraved in a thin metal film deposited on the surface of a piezoelectric crystal, as illustrated in Figure 1. When a radio frequency voltage source is applied between the electrodes, a SAW standing wave is generated which decomposes into travelling waves in the +x and the -x directions. Thus, this transducer is bi-directional and it will also detect SAWs that are incident from either direction.

Each gap between electrodes of opposite polarity can be viewed as as an individual SAW source. The strength of each source can be "weighted" by varying the overlap region within the acoustic beam. The entire transducer can be modelled as an array of SAW sources with alternating polarity on a SAW transmission line as shown in Figure 1. The SAW amplitude at any point is given by a sum over the individual sources, each multiplied by an appropriate phase factor. In fact, the source strength is itself a function of frequency and electrode configuration, and the sources are not independent. Except for these important (but calculable) effects, the SAW filter is an ideal transversal filter. This result allows the SAW device designer to utilize the powerful transversal digital filter design algorithms as the nucleus of a SAW filter design method.

The center frequency of the simple filter in Figure 1 is $f_o = v_s/2p$, where v_s is the SAW velocity and p is the center-to-center electrode spacing. Operation at harmonics of f_o can also be obtained, thereby reducing photolithographic reso-

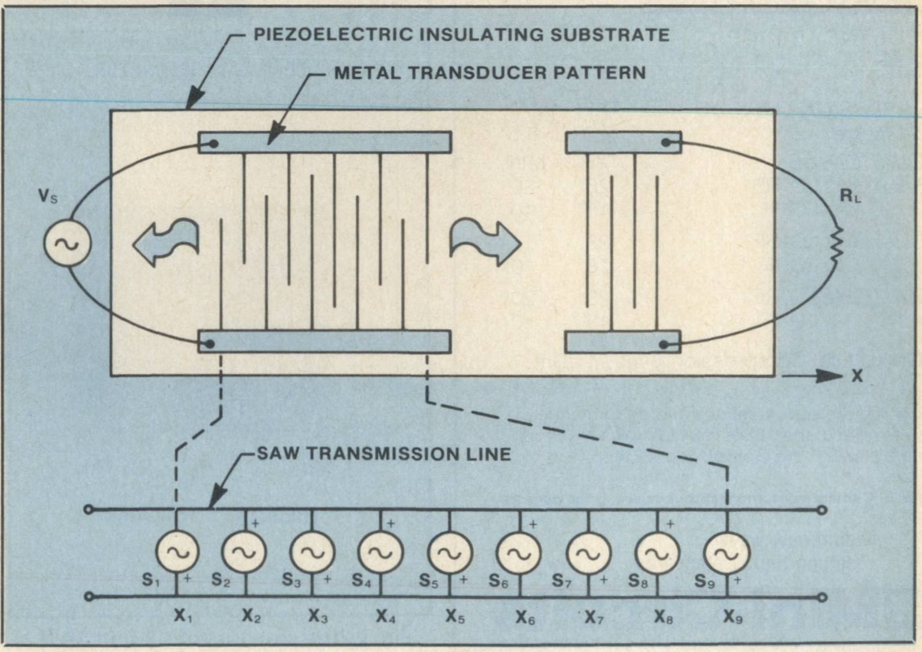

Fig. 1 The basic SAW interdigital transducer and its simplified equivalent circuit.

[*Continued on page 74*]

[From page 73] **SAW DEVICES**

lution requirements for high frequency devices. However, the harmonic response is degraded by non-ideal effects, most notably by the propagation of bulk acoustic modes.

—Reflective Array Devices

A metal film on the surface of a piezoelectric crystal perturbs the electrical boundary conditions and results in a perturbation of the SAW velocity that causes reflections at the edges of the transducer electrodes. The reflections within a transducer interfere constructively in a "stop-band" that has a center frequency determined by $v_s/2p$ and a bandwidth proportional to the length of the transducer and the reflection coefficient of each electrode. Within this "stop-band" the reflections can cause severe distortion of the transducer response. However, the transducer period can be decreased, thereby moving the "stop-band" to a higher frequency and reducing the severity of the effect. The two most important types of reflective SAW devices are the reflective array compressor (RAC) for radar pulse compression filters, and the SAW resonator for narrowband bandpass and frequency control devices. Both of these devices use standard interdigital SAW transducers for generation and detection, but the primary signal processing functions are accomplished by the reflective gratings.

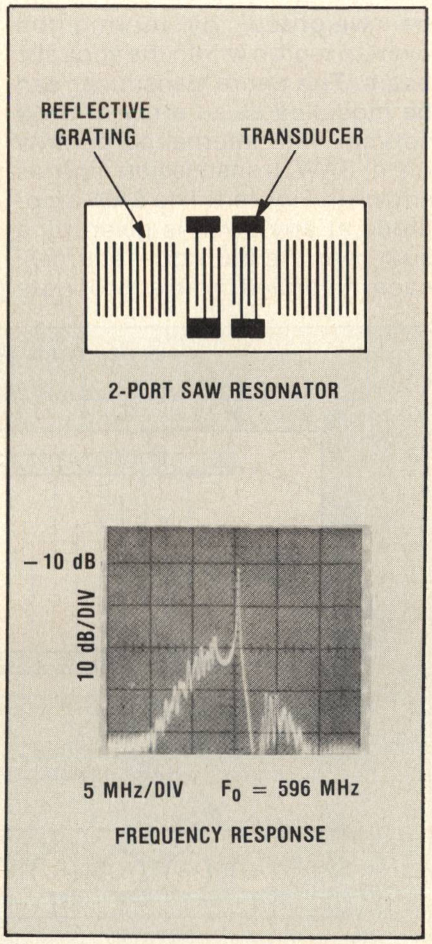

Fig. 2 The structure of a 2-port SAW resonator and its typical frequency response.

For example, the SAW resonator shown in Figure 2 consists of one or more transducers positioned between two reflective gratings. Within the "stop-band" the gratings act like high reflectivity mirrors forming a Fabry-Perot type resonator. As shown in the figure, the transmission response between the two transducers of a two port resonator is characterized by a narrow peak at the resonance frequency of the SAW cavity superimposed on the direct transducer response.

The bandwidth of the transmission response is now controlled by the Q of the SAW cavity rather than the bandwidth of the coupling transducers. The unloaded Q of a SAW resonator depends most heavily on the acoustic propagation loss. The relationship between loss and Q is given by

$$1/Q = \propto v_s/\pi f_o$$

where $\propto$ is the propagation loss in nepers/cm and f_o is the resonance frequency.

Bandpass Filters

All SAW devices are inherently bandpass filters; high pass and low pass units are not possible. The challenge of SAW filter design is to incorporate corrections for non-linear responses so as to achieve the desired filter response. This complex task is typically performed by employing interactive numerical techniques that (usually) converge to an acceptable solution which prescribes a specific transducer topology.

Figure 3 illustrates the three most important transducer weighting schemes on which SAW bandpass filter designs are based. Figure 3a shows the "overlap" weighting technique described previously. Note that the resulting SAW amplitude is nonuniform perpendicular to the propagation direction and, the weighting is only effective if the SAW energy is "averaged" across the acoustic beam. Thus, both transducers in a simple SAW filter cannot be overlap weighted, since neither averages the SAW profile of the other.

Figure 3b illustrates a means of accomplishing weighting while maintaining a uniform overlap. This technique, termed "withdrawal" weighting, results in a lumped approximation to a desired weighting function by varying the density of driven electrodes in a uniform transducer. The accuracy of the approximation depends on the number of electrodes in the transducer, thus it is most advantageously employed in filters having narrow fractional bandwidths or very small shape factors.

Another technique, illustrated in Figure 3c, utilizes the dependence of source strength on electrode width and spacing to achieve source weighting. This technique

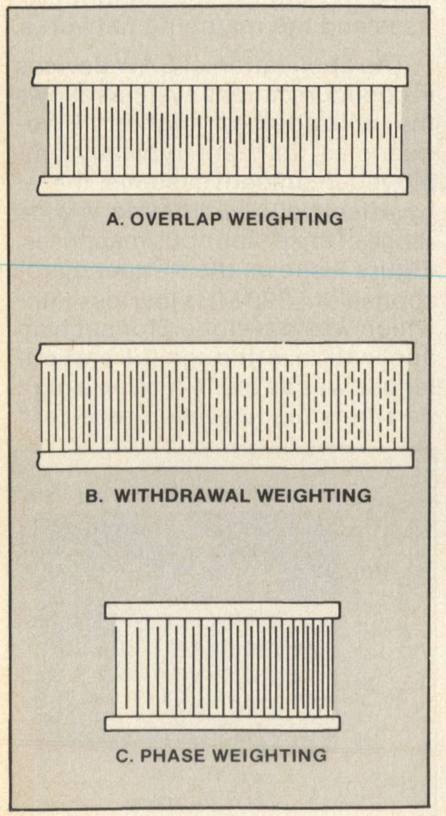

Fig. 3 SAW transducer weighting techniques.

[Continued on page 76]

[From page 75] **SAW DEVICES**

is termed "phase" weighting and, like the previous method, maintains uniform overlap. The disadvantage is that it introduces weighting of the phase response due to the varying periodicity that must be compensated in the other transducer in linear phase filters. This weighting technique is primarily employed in dispersive pulse compression filters.

The bidirectionality of these basic "two-phase" transducers results in an intrinsic inefficienty that causes an extra 6 dB of insertion loss, above that determined by input and output impedance considerations. In addition, it results in multiple reflections between the transducers that cause distortion in the desired response. In practice it is usually necessary to introduce at least 20 dB of insertion loss to attenuate these reflections. By employing three or more phases, and incorporating suitable matching networks, a transducer can be realized that generates a single travelling wave, and is therefore unidirectional [1]. This obviates both limitations, at the expense of substantial complications to both the fabrication process and the matching networks.

The application of SAW devices in communications systems allows the utilization of higher IF frequencies than are typically employed in present systems, thereby effectively eliminating a wide range of mixer spurious responses. Figure 4 shows the frequency response of a 328 MHz low loss filter which was developed for such an application. Although the particular use was as the IF filter in a high performance television receiver [2]

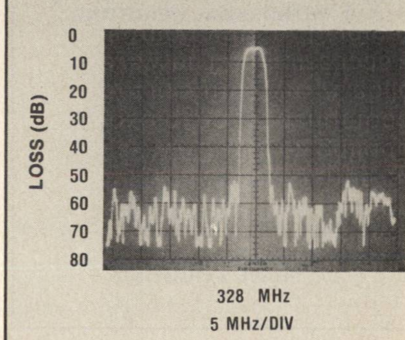

Fig. 4 A high performance 328MHz experimental TV-IF filter.

having an IF frequency eight times higher than in current TV receivers, the concept is applicable to military communications systems. This filter utilizes a three-phase transducer structure to achieve 6 dB insertion loss simultaneously with 50 dB triple transit suppression. The weighting of the filter uses a combination of phase weighting and withdrawal weighting. The filter also includes phase and magnitude compensation for distortion effects of the three phase matching network, notch filters in both baseband and IF sections of the television receiver, and predistortion of television transmitters. This filter provides greatly improved rejection of signals from adjacent channels compared to current receivers. The low loss of the filter allows the receiver to achieve an excellent noise figure with greatly improved interference rejection. Widespread utilization of this TV receiver architecture could lead to an easing of the current restriction on the utilization of 18 UHF TV channels for each assigned channel.

Figure 5 shows an L-band filter fabricated on ST-cut quartz for temperature stability at a center frequency of 1575.4 MHz for the global positioning system manpack receiver [3]. This filter utilizes both overlap and withdrawal weighted unidirectional transducers and exhibits excellent out-of-band rejection over a wide bandwidth The phase response of this filter varies about ±3% over the 1 dB bandwidth, and the delay variation is less than 10 ns.

Table 1 is a presentation of the electrical capabilities of SAW bandpass filters, indicating present and projected limits. Note that design trade-offs are necessary between certain parameters; all of the indicated limits cannot be achieved simultaneously.

Fractional bandwidths less than 0.1% require transversal filters having transducers with thousands of electrodes. For this purpose, SAW resonators can be coupled electrically or acoustically to realize multipole narrow band filters that are compact and easily designed using well known techniques [4]. Figure 6 shows the response of a two-pole resonator filter designed to give a Butterworth response with a 3 dB bandwidth of 14 kHz at a center frequency of 184 MHz [5]. The unloaded Q of the component resonators was about 20,000.

Frequency Control

Both SAW delay lines and resonators can be utilized as frequency control components in oscillator circuits.

The choice of the delay lines vs. the resonator approach currently depends on the frequency range of interest. The effective Q of the delay line is determined by its

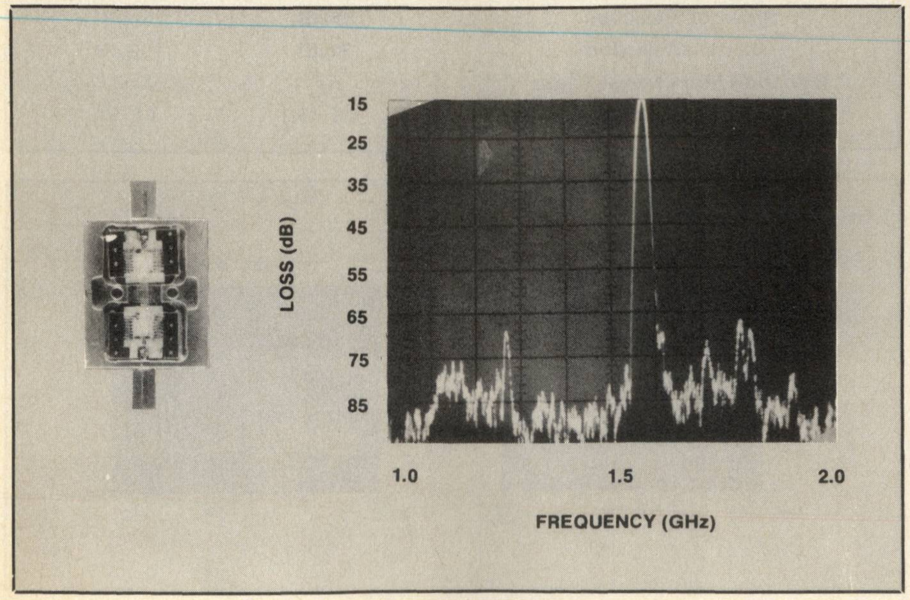

Fig. 5 An L band front end filter used in GPS.

[*Continued on page 78*]

[*From page 77*] **SAW DEVICES**

group delay and is approximately

$$Q_{\text{delay line}} + \pi f_o L / v_s$$

where f_o is the oscillator frequency, L is the delay line length and v_s is the SAW velocity. The advantage of the delay line approach is that 3rd harmonic transducer operation can be utilized, thereby substantially easing photolithographic requirements, whereas the resonator suffers a dramatic reduction in Q due to SAW to bulk mode conversion at the 3rd harmonic.

The absolute accuracy of the oscillator center frequency depends on the accuracy of crystal orientation and control of fabrication processes. However, the frequency can be trimmed by adjusting the thickness of the transducer metallization.

Noise performance of SAW oscillator is typically better than for bulk crystals, primarily due to the higher power handling capabilities of the SAW device [6]. The aging characteristics of SAW oscillators result in variations that are typically 1 to 10 ppm/year, about an order of magnitude worse than the best bulk devices, and critically dependent on substrate surface cleanliness and device packaging [7].

The best temperature stability for SAW oscillators without external compensation is obtained on ST-quartz which has a vanishing first order temperature dependence of delay (length/velocity). The observed dependence is quadratic, and resuslts in a variation of about 150 ppm over the mil-spec temperature range. This variation is substantially larger than measured for bulk devices, and constitutes the most serious deficiency in high performance SAW oscillators. Numerous techniques for externally improving the temperature performance have been reported in the literature, all requiring either extra parts, power, and space, or substantially complicating the fabrication process. A recent review of these techniques is presented in [8].

Radar Applications

Perhaps the most significant impact surface wave devices have

TABLE 1
SAW FILTER CAPABILITIES

PARAMETER	PRESENT	PROJECTED
Center Frequency (f_o)	10 MHz to 4.4 GHz	6 GHz
Bandwidth	20 KHZ to .7 f_o	.8 f_o
Insertion Loss	2 dB	1 dB
Minimum Shape Factor	1.2	1.2
Minimum Transition Bandwidth	50 KHz	20 KHz
Sidelobe Rejection	60 dB	70 dB
Ultimate Rejection	90 dB	100 dB
Deviation From Linear Phase	±1°	±.5°
Amplitude Ripple	.01 dB	.01 dB

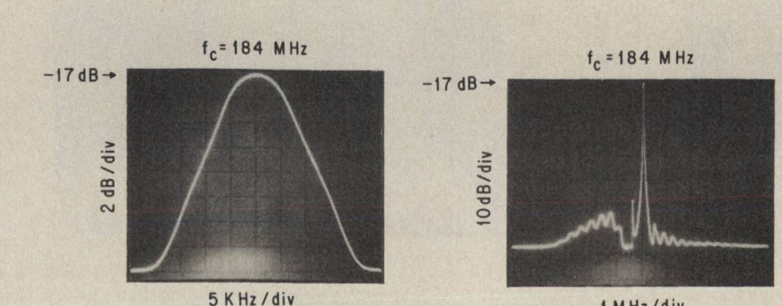

Fig. 6 An electrically coupled 2-pole SAW resonator filter.

made on military systems is the improvement in radar systems performance made possible by SAW pulse compression filters (PCF). A figure of merit in pulse compression systems is the time-bandwidth product (TB) of the transmitted waveform. The system exhibits an equivalent noise bandwidth equal to 1/T where T is the transmitted pulse width in seconds. The radar range resolution is approximately c/2B where B is the waveform bandwidth in hertz and c is the speed of light (3 x 10^8m/s.)

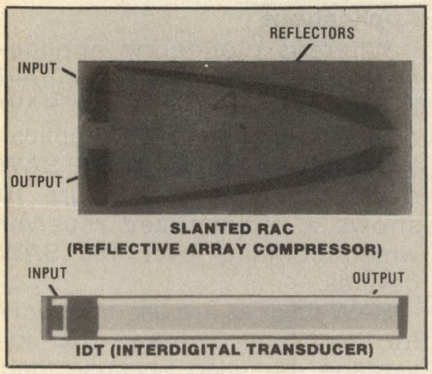

Fig. 7 SAW pulse compression filters.

Prior to SAW technology, a chirped transmitter waveform was generated using a ramp driven linear voltage controlled oscillator and matched filtering was accomplished in the receiver using dispersive lumped and distributed element filters such as the folded tape meander line (FTML). The use of SAW filters is the exciter (transmitter) and receiver has eliminated expensive alignment procedures, provided a limitless choice of waveforms and added an extra dimension is system design due to the excellent reproducibility of SAW devices that permits the realization of multichannel processors.

Both the reflective array compressor (RAC) described previously, and the transversal filter have been utilized in this application, and representative examples are shown in Figure 7. Some of the more important classes of waveforms that have been realized using SAW devices are the Hermitian [9] which has a rotationally invariant ambiguity function, the doppler insensitive waveforms observed in bats [10], and the general class of FM waveforms which have uniform envelopes at the transmitter and are compatible with high power amplifiers.

Figure 8 compares the performance of two waveforms from the FM class: linear FM (LFM) and nonlinear FM (NLFM). Both have "flat" time domain responses, however, inspection of the spectrum of the transmitted signal for the NLFM device shows it to be smooth and without the Fresnel ripple observed on the LFM device.

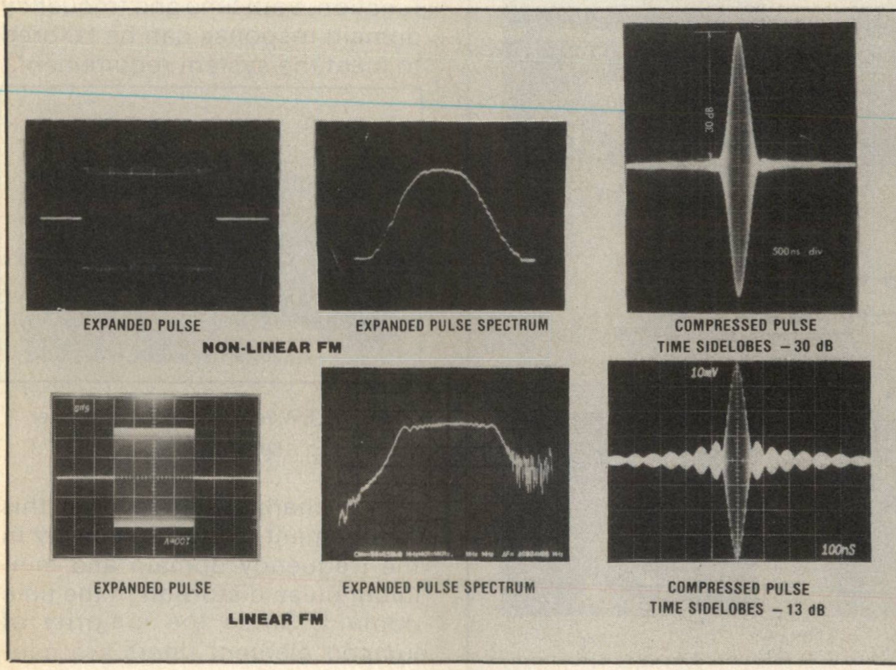

Fig. 8 Performance comparison of linear FM and nonlinear FM SAW compression filters.

[*Continued on page 80*]

The importance of the NLFM waveform is observed when the signal is compressed in the PCF and the maximum signal to noise improvement is realized [maximum S/N is equal to 10 log (TB)] *without* generating large time sidelobes. Linear FM is much less sensitive to doppler than NLFM but time sidelobes must be suppressed by amplitude weighting the PCF power spectral density (as compared to phase weighting in NLFM) and the price paid is a degradation of receiver sensitivity by typically 1 to 1.5 dB.

An important class of radar systems is the monopluse radar in which target tracking information is obtained from a single pulse [11]. The significance of SAW devices in these systems (in addition to pulse compression) is the ability to match amplitude and phase characteristics of several devices in the time domain, the frequency domain, and over temperature. Amplitude and phase tracking is typically demonstrated by inspecting frequency domain data, however, device performance perceived by the radar operator depends on time domain characteristics.

Figure 9 illustrates the concept. Two 20us expanded pulses enter the PCF in the dual channel receiver and produce 300ns compressed pulses at the output. The phase processor produces sum (Σ) and difference (Δ) signals from which tracking information is derived. If a point target is located on boresight, the Σ signal should be 6dB greater than a single channel signal, and the Δ signal should vanish. As shown in the figure, the Σ/Δ ratio in this system is about 45dB. Not only is the "main lobe" canceled in the Δ channel, but time sidelobes are reduced as well, indicating tracking of time spuria between devices.

Radar systems have been developed that exhibit extremely high range resolution: on the order of one foot. This requires that the operational bandwidth be a minimum of 500MHz.

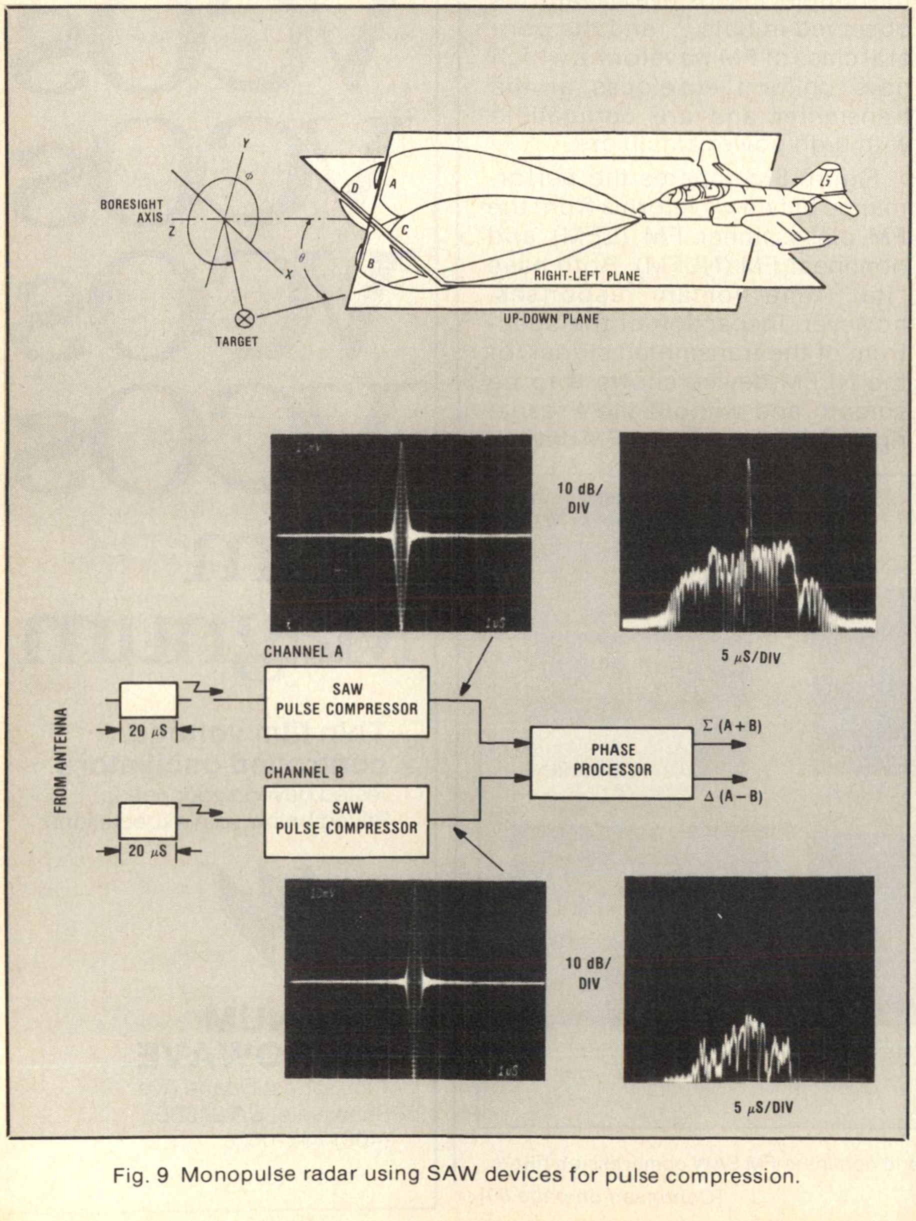

Fig. 9 Monopulse radar using SAW devices for pulse compression.

Electronic Warfare (EW) Applications

Whereas pioneering applications of SAW technology occurred in radar requiring 10 to 20 SAW devices per system, EW applications may employ 50 to 500 SAW devices per system! Figure 10 shows a channelized receiver which contains over 160 SAW devices.

SAW devices are used not only for their small size and cost advantage, but also because their performance surpasses that of most competing technologies. This performance results from the superior phase linearity which can be realized with SAW devices that is critical for the pulse analysis performed in channelized receivers. Since SAW devices ideally implement the transversal filter function, both time and frequency domain response can be tailored to meet the system requirement.

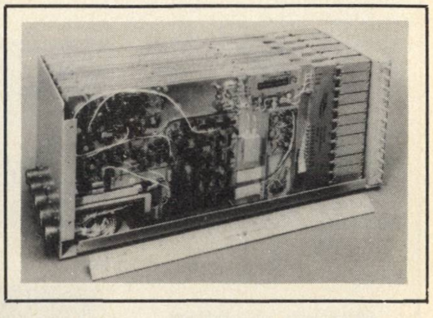

Fig. 10 EW receiver employing over 160 SAW filters.

In a channelized receiver this requirement is high selectivity in the frequency domain and minimum pulse distortion in the time domain. Since the majority of lumped element filters are minimum phase, infinite impulse response designs, the phase re-

[*Continued on page 82*]

sponse at the band edges is distorted and results in a response to out-of-band pulses that "rings" for a substantial interval. SAW transversal filters, on the other hand, are finite impulse response devices that can exhibit extremely linear phase response with optimum response to out-of-band pulses.

The cued receiver diagram shown in Firgure 11 consists of a channelized receiver containing a bank of SAW bandpass filters and an analog memory. Input signals are applied simultaneously to the channelized receiver and to the input of a wide bandwidth SAW delay line. The channelized receiver determines coarse signal frequency, even in the presence of other simultaneous signals, and directs a narrow-band receiver to perform detailed analysis of the signal as it emerges from the delay line.

The bandpass (slot) filters have a 3dB bandwidth of 20MHz and uniformly spaced center frequencies that provide an instantaneous receiver bandwidth of 700MHz. The slot bandwidth is

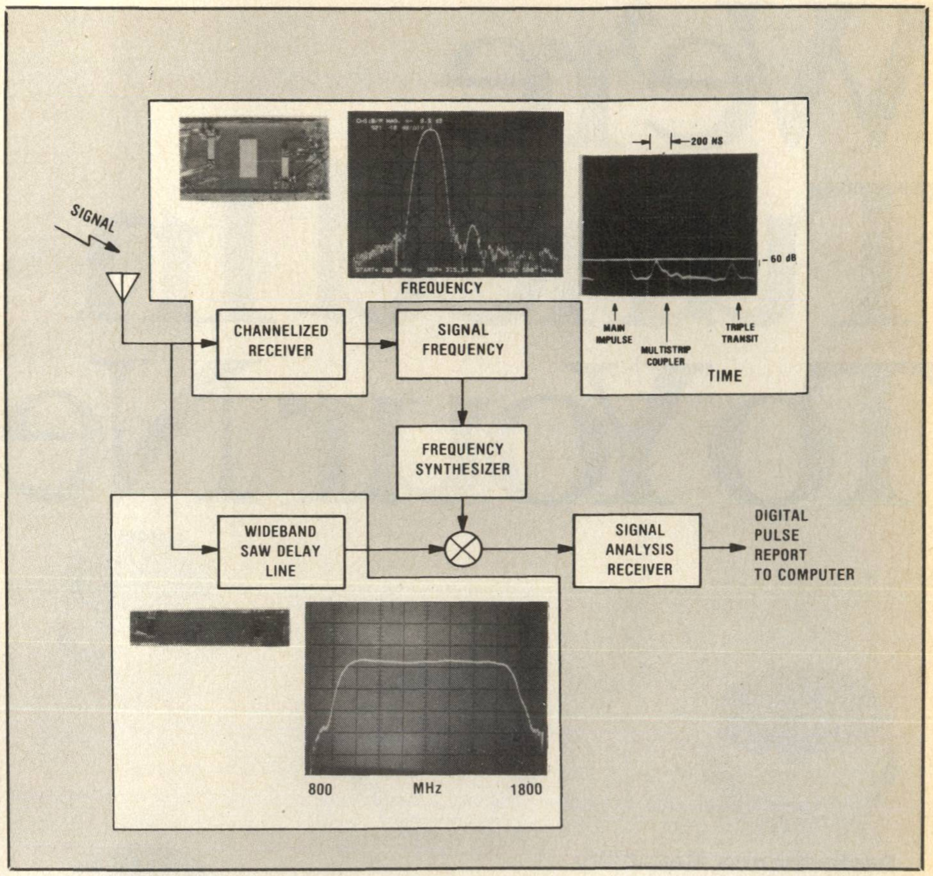

Fig. 11 Cued analysis receiver architecture.

[Continued on page 84]

dictated by video processor circuitry that must detect 100ns pulses economically with an instantaneous dynamic range of 60dB. Undirectional 3-phase technology is used for these filters to eliminate multiple-transit echos, with an additional benefit of low insertion loss.

Microscan receivers are less complex than cued analysis receivers, however, they are limited in instantaneous dynamic range (typically 30dB) by time sidelobes. Figure 12 illustrates the operation of a microscan receiver. These systems use LFM PCF devices exclusively to accomplish an operation that is equivalent to the digital chirp Z-transform [12]. The bandwidth of the SAW devices in such systems is typically 1 GHz with TB of 100 resulting in a resolution of 10MHz. Video circuitry capable of processing such wide bandwidth signals borders on the state-of-the-art.

The SAW Convolver

Military systems are evolving to counter the threat of hostile jammers or to operate covertly to avoid detection by hostile receivers. These systems require a matched filter with high processing gain (>30dB) and waveform agility. The latter is also applicable to encryption requirements in secure communications systems. A schematic representation of a monolithic elastic SAW convolver that exhibits these features is shown in Figure 13.

The convolution results from non-linearities in the elastic properties of the substrate such that two counter-propagating waves are effectively multiplied spatially, and the spatial product is integrated over the interaction length by a simple parallel plate electrode. In this device, the input and reference waveforms are modulated on a 300MHz IF, and the convolved output occurs at 600MHz. The figure demonstrates convolution of a 20us pseudorandom sequence having a 100MHz bandwidth with its time reversed reference producing a 5ns compressed pulse.

Devices have achieved 32dB of processing gain with a 1dB implementation loss and an instantaneous dynamic range of 60dB. This low cost programmable matched filter, realized by a simple aluminum metallization on a $LiNbO_3$ substrate, has the equivalent processing power of a 10-bit digital processor performing $2x10^{11}$ complex multiplies and adds per second.

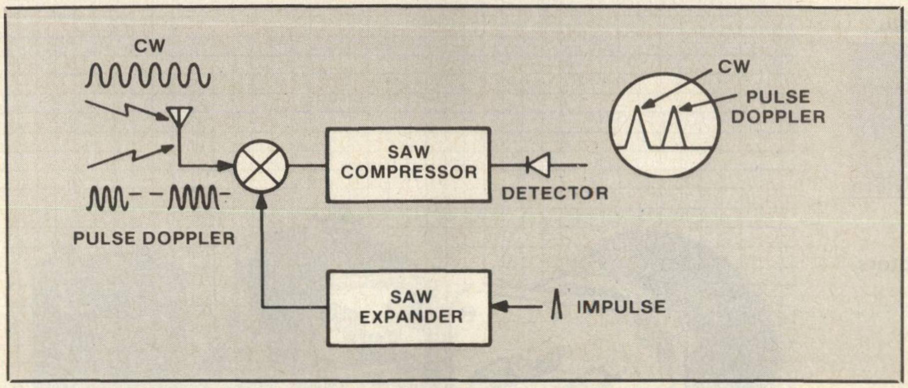

Fig. 12 Simplified block diagram of microscan receiver.

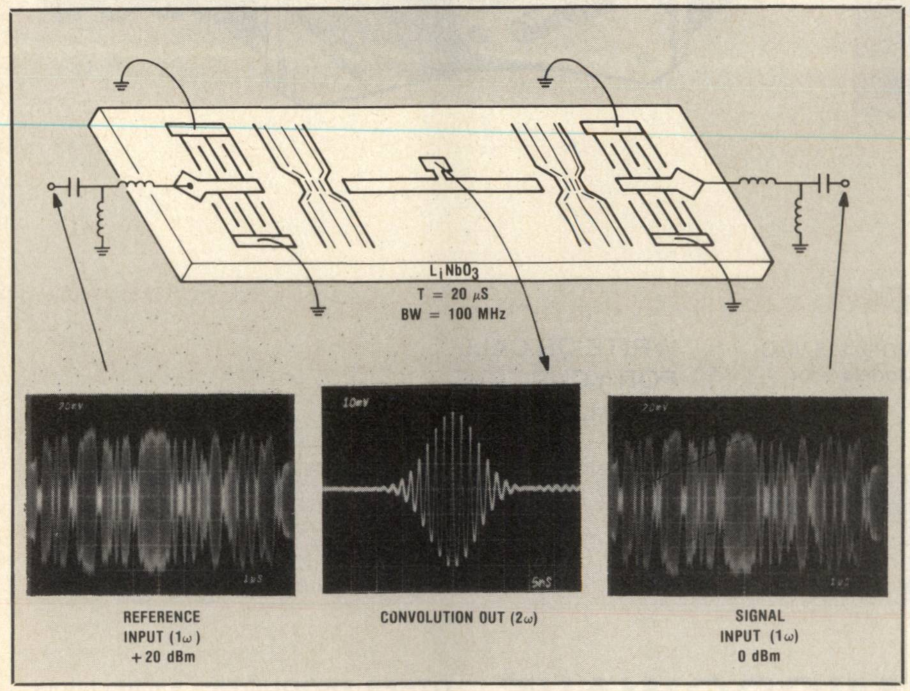

Fig. 13 The SAW convoler as a programmable matched filter.

Conclusions

The maturity of SAW device technology is due, in large part, to the early stimulus of special applications in military systems. Current applications are diverse, ranging from high performance band pass filters having low insertion loss and excellent out-of-band rejection to devices capable of performing powerful analog signal processing functions. This range of applications will most certainly broaden as research produces improvements in substrate materials, fabrication techniques, and the understanding of device physics.

REFERENCES

1. Rosenfeld, R.C., R.B. Brown, and C.S. Hartmann, "Unidirectional Acoustic Surface Wave Filters with 2dB Insertion Loss," in *1974 Ultrasonics Symposium Proceedings*, IEEE Publication No. 74CH0896-1SU, pp. 425-428, Nov 1974.
2. Ash, D.L., "High Performance Receiver," IEEE Trans. Consumer Elect. Vol. CE-24, No. 1, pp. 39-46, Feb. 1978
3. Potter, B.R. and D.B. MacDonald, "SAW Filter Technology and Applications," in *Proceedings of the 1981 Frequency Control Symposium*, May 1981
4. Zverev, A.I., *Handbook of Filter Synthesis*, John Wiley and Sons, New York 1967.
5. Ragan, L.H., "Surface Acoustic Wave Resonator Rilter," 1976 IEEE International Microwave Symposium, (unpublished).

[*Continued on page 86*]

[From page 84] **SAW DEVICES**

6. Pevavaire, L., et al., "A 120MHz SAW Resonator Stablized Oscillator with High Spectral Purity," in *1980 Ultrasonics Symposium Proceedings*, IEEE Publications No. 80CH1602-2, pp. 256-259, Nov. 1980.
7. Parker, T.E., "Analysis of Aging Data on SAW Oscillators," in *Proceedings of the 1980 Frequency Control Symposium*, pp. 292-301, May 1980.
8. Lewis, M., "Temperature Compensation Techniques for SAW Devices," in *1979 Ultrasonics Symposium Proceedings*, IEEE Publications No. 79CH1482-9, pp. 612-622, Sept. 1979.
9. Klauder, J.R., "The Design of Radar Signals Having Both High Range Resolution and High Velocity Resolution," Bell Sys. Tech. Journal, pp. 809-820, July 1960.
10. Titlebaum, E.L., "Echolocation Systems in Nature; A Theory of Optimum Insensitivity to Motion for Bats," in *1978 Ultrasonics Symposium Proceedings*, IEEE Publications No. 78CH1344-1, pp. 1-7, Sept. 1978.
11. Skolnik, M.I., *Radar Handbook*, Mc-raw-Hill, New York, 1970.
12. Rabiner, L.R., R.W. Schafer, and C.M. Rader, "The Chirp Z-Transform Algorithm," IEEE Trans. on Audio and Electroacoustics, Vol. AU-17, pp. 86-92, June 1969

Clinton S. Hartmann, *Mr. Hartmann received the B.S. degree in Electrical Engineering from the University of Texas, Austin, in 1967. He received the S.M. and E.E. degrees from the Massachusetts Institute of Technology, Cambridge, in 1968 and 1969, respectively.*

Mr. Hartmann has been Chief Executive Officer of RM Monolithics, Inc. since co-founding the company in 1979. He was previously employed at Texas Instruments where he had attained the position of Research Fellow in recognition of his fundamental contributions in the field of Surface Acoustic Wave devices. In 1976 he was named the Outstanding Young Electrical Engineer in the United States by Eta Kappa Nu.

Mr. Hartmann is the inventor of several SAW devices which are in common use today. He holds fundamental patents on the low loss surface wave filter, the SAW resonator, the SAW controlled oscillator, and many others. He holds more than 30 patents in this area. He was co-winner of the 1970 Outstanding Paper Award of the IEEE Transactions on Sonics and Ultrasonics. He has taught short courses on SAW design at Massachusetts Institute of Technology, Purdue University, George Washington University, and the National Electronics Conference. He was Microwave Acoustics editor for the IEE Group on Microwave Theory and Techniques in 1978.

Mr. Hartman is a member of Tau Beta Pi, Eta, Kappa Nu, Sigma Xi, and the IEEE.

Robert J. Kansy, *Robert Kansy received the B.S., M.S., and Ph.D. degrees in Electrical Engineering from the University of Illinois at Urbana-Champaign in 1970, 1971 and 1975, respectively.*

Dr. Kansy joined RF Monolithics in 1980 and is Director of Surface Acoustic Wave Research and Development. His responsibilities include performing fundamental analyses of new SAW device configurations, simulating device performance using computer-aided techniques, and developing device design software.

Previously, Dr. Kansy was a Member of the Technical Staff in Texas Instruments' Central Research Laboratories where he contributed to the development of charge-coupled device technology in HgDcTe for applications in infrared imaging systems. His earlier association with TI's Equipment Group involved the design and development of several silicon integrated circuits using n-channel MOS/CCD technology for analog signal processing applications in radar and infrared imaging systems. Prior experience at the Magnavox Corporation included the design of SAW filters for military and consumer applications.

W. D. Daniels, *Mr. Daniels received the B.S. and M.S. in Electrical Engineering from the University of Alabama. He is a Member of the Technical Staff and is manager of the Acoustic Signal Processing of the Microwave Laboratory of the Equipment Group at Texas Instrumments. He joined TI in 1972 as a surface wave device design engineer and was responsible for some of the fundamental SAW development at Texas Instruments which included such devices as bandpass filters, tapped delay lines, pulse compression filters, and code correlators. His microwave component design work includes X-band multipliers, mixers, couplers, and filters. In 1976 he became the project engineer responsible for the development of the first channelized receiver using 144 unidirectional SAW filters. The design and integration of this receiver required design in digital, RF, IF, and video circuit disciplines. At the close of this program, Mr. Daniels was given the responsibility for concept development, design, and execution of the Dual-Mode program. This system used a high accuracy [4-mrad] wideband RF seeker boresighted with an imaging infrared seeker.*

B. R. Potter, *Mr. Potter received the B.S. and M.S. degrees in Electrical Engineering from California State University and Brigham Young University, respectively. He is a Member of the Technical Staff in the SAW Branch of the Microwave Laboratory of the Equipment Group at Texas Instruments. In this assignment, he has been responsible for several challenging SAW device programs such as L-band SAW filters for the Global Positioning System satellite. He is also responsible for directing the work of a number of other SAW research and development engineers and technicians. Previously, Mr. Potter was a research engineer in the Central Research Laboratories, where he was responsible for major developments in low-loss SAW filters and linear FM slanted correlators. Previous work at Varian Associates and General Dynamics included microwave filters, diplexers, couplers, and system modelling for MTI radars.*

Mr. Potter is a member of the IEEE, Eta Kappa Nu and Tau Beta Pi, and is the author of papers on microwave travelling wave tubes, low-loss SAW filters and slanted correlators. ■

[From page 58] MMIC

Further anticipating, John says, "learning curve" isn't going to help either. Learning curve implies that prices come down as you make lots of devices spread out over long periods of time with essentially no changes made to the product. "This isn't the microwave way," says John, "Nothing remains unchanged in microwave designs long enough for the learning curve to help out." Further capping his pessimistic MMIC thesis, John points to the lack of adequate microwave professors in the academic community, noting that you can count the number of them in the entire country easily. This, says John, doesn't speak well for the hope for learning curve that MMIC proponents dream about.

What's John's bottom line? "GaAs MMIC's will be used to make those things you can't make otherwise! They'll go into very expensive systems wherein their high component value will be buried."

Comments From The Floor

Whether Saloom and his panellists speak with tongues forked or in cheek we do not know for sure. What can be said is that they ellicit the obvious desired response from the floor.

Bert Berson volunteers that if GaAs IC's were available, lots of new applications would explode to life, not the least of which would be the 10 million X-band direct satellite broadcast receivers that the world's TV viewers "need."

Also advanced is the theory that during the development of monolithic silicon circuits, the hand calculator, one of its most prolific children, wasn't even envisioned (sic the value of such projections, including those made today).

Joe Saloom, introduced as the Illinois born, raised and educated industrialist and philosopher, closes by saying that he has faith in the microwave profession and in its ability to be ingenious in raising money and devising new ideas to take advantage of a technology which that profession so obviously loves. ■

Waveguide Filters for mm Wavelengths

John Bratherton
MM Microwave Ltd.
N. Yorks, England

Millimeter-waves span more than 3 octaves of frequency from around 30 GHz to over 300 GHz, accounting for nearly half the entire microwave spectrum. Although the majority of this band is affected significantly by atmospheric attenuation, limiting it to short or medium range use in a terrestrial environment, it nevertheless offers enormous potential for development. Interest and activity in millimeter-waves have been increasing gradually over the last few years and, as component technology improves, applications are emerging at a growing rate. It seems clear that by the end of the decade millimeter-wave systems will be seeing extensive use and will represent an important part of the output of the microwave industry.

Amongst the many applications reported to date, communications play a prominent part. Freedom from the congestion of the lower frequency bands together with the increased channel space available favor the millimeter-wave for short to medium-haul systems, whilst small high-gain antennas at these frequencies provide an attractive proposition for mobile links. Also there are possible applications for secure communications utilizing the high atmospheric absorption peaks which occur in the band. Military applications include weapons guidance, target detection and terminal homing where the light compact equipment is an advantage. Battlefield surveillance radars benefit from the superior performance of millimeter-waves over infrared in conditions of poor visibility. Radio astronomers have begun important new work in millimeter-wave spectrometry, and there are research applications connected for example with particle accelerators and plasma diagnostics. Recently reported are traffic control systems and various industrial process control applications.

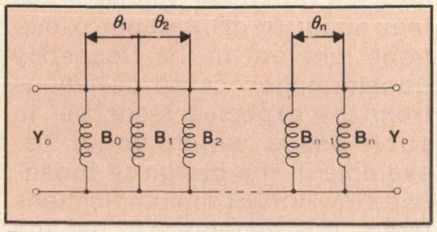

Fig. 1 Equivalent circuit of direct-coupled cavity filter.

To meet the growing demand for millimeter-wave components, researchers and component designers have been exploring the high frequency possibilities of different forms of transmission line such as dielectric waveguide, finline structures and suspended substrate microstrip, whilst at the high-end of the millimeter-wave spectrum some interesting quasi-optical techniques are under investigation. All these media have their own merits under certain circumstances, offering a measure of intergrability and choice. Nevertheless the systems designer has to satisfy multiple and sometimes conflicting criteria in the selection of components often on the basis of compromise, and many systems will contain a mixture of technologies. Conventional waveguide may well be the most appropriate choice in many cases, and there is no doubt that waveguide components will continue to play an important role in millimeter-wave systems at least up to 140 GHz. In particular waveguide filters can offer significant performance advantages in the most stringent applications. The purpose of this article is to describe a development program aimed at the design and production of direct-coupled waveguide filters, initially in Ka-band , using techniques which are directly applicable at frequencies up to 140 GHz. The design method, realization and production considerations are discussed together with predicted and experimental results for a bandpass filter centered around 37.5 GHz which is now in quantity production.

The Problem

Figure 1 shows the equivalent circuit of a direct-coupled cavity filter consisting of shunt inductive suspectances B_i separated by lengths of transmission line θ_i.

When the transmission line is to be formed from waveguide, the filter designer must answer 3 basic

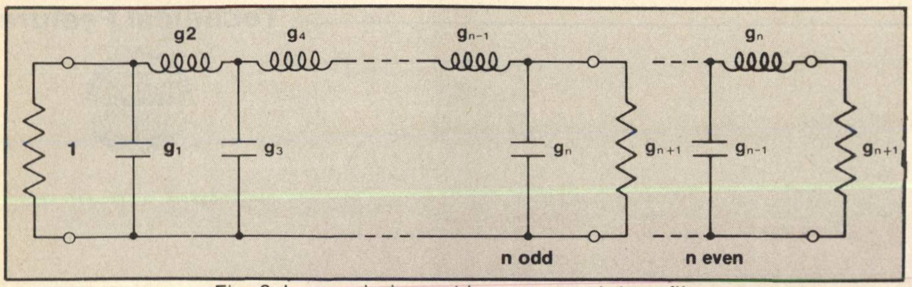

Fig. 2 Lumped-element low-pass prototype filter.

questions:

(i) What are the theoretical values of B_i and θ_i to obtain the desired filter response?
(ii) How can these values be achieved in waveguide in an accurately predictable way?
(iii) Is it possible to produce the resultant structure with realistic manufacturing tolerances; will it need to be tunable after assembly and if so, how?

The answers to questions (ii) and (iii) become particularly pertinent at higher frequencies, and for millimeter-wave filters they are crucial. The realization question posed in (ii) is discussed in detail, but first some useful comments can be made concerning the design question (i).

Filter Design

The theory of direct-coupled-cavity filters is well established in the literature, and the filter designer has a choice of several methods. The author employs one of two well known techniques depending on filter specification.

Cohn[1] based his theory on a lumped-element low-pass prototype as shown in Figure 2.

The element values g_i of this prototype determine the type of response obtained and can be found from published tables[2] for maximally flat (Butterworth) response or Tchebysheff (equal ripple) response. Alternatively they can be calculated for intermediate ripple values or different types of response which aré not tabulated[2]. Having determined the element for the low-pass prototype, a low-pass to band-pass transformation is carried out leading to simple design formular which are still widely used. An example of a low-pass prototype response together with its transformed band-pass equivalent are shown in Figure 3 for the case of a 5-section Tchebysheff filter. Cohn's design equations are also given.

Cohn's method works very well for filters with narrow bandwidth or relatively high ripple values, predicting band-edge frequencies, skirt attenuation and VSWR quite closely. However for bandwidths of greater than 1 or 2 percent coupled with ripple values of less than about .05 dB, the approximations inherent in the frequency transformation cause deviations from the expected response. In such cases which occur for example in the design of broadband low-VSWR communications filters, it is necessary to use the method developed by Levy[3] based on a distributed low-pass prototype filter. The form of this prototype is shown in Figure 4.

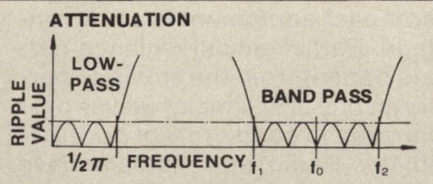

$$\frac{B_i}{Y_0} = \frac{1}{\Omega\sqrt{g_i g_{i+1}}}\left[1 - \frac{(\Omega^2)}{g_i g_{i+1}}\right] \quad i = 0, 1, 2 \ldots n$$

$$\theta_i = \pi - \frac{1}{2}\left[\cot^{-1}\frac{B_{i-1}}{2Y_0} + \cot^{-1}\frac{B_i}{2Y_0}\right]$$

$i=1,2 \ldots n$

where $\Omega = \pi \dfrac{\lambda g_1 - \lambda g_2}{\lambda g_1 + \lambda g_2}$

$$g_0 = \Omega, \quad g_{n+1} = \frac{\Omega}{R}$$

and λ_{g0}, λ_{g1}, λ_{g2} are the guide wavelengths corresponding to frequencies f_0, f_1, f_2.

Fig. 3 Low-pass to band-pass transformation and design formular for lumped-element prototype filter.

This time the response of the prototype is determined by the step impedances Z_i which are obtained directly from Levy's tables.[4] The low-pass to band-pass transformation then yields the design formular:

$$\frac{B_i}{Y_o} = \frac{Z_i - Z_{i+1}}{\sqrt{Z_i Z_{i+1}}} \text{ for } Z_i > Z_{i+1} \quad i=0,1,2 \ldots n$$

and

$$\frac{B_i}{Y_o} = \frac{Z_{i+1} - Z_i}{Z_i Z_{i+1}} \text{ for } Z_i < Z_{i+1} \quad i=0,1,2 \ldots n$$

$$\theta_i = \pi - \frac{1}{2}\left[\cot^{-1}\frac{B_{i-1}}{2Y_o} + \cot^{-1}\frac{B_i}{2Y_o}\right] \quad i=1,2 \ldots n$$

Although capable of superior results for broadband filters, this method is not nearly so easy to use as Cohn's. The published tables of step impedances, though extensive, are not sufficiently detailed to cover all filter requirements, particularly those with a large number of sections in the medium bandwidth bracket. This is precisely the combination called for by many communications filters, and hence it is necessary to derive the step impedances for these cases. The process requires computer calculations of great precision, although the synthesis as described by Levy[4] does contain a measure of self-checking.

It is worthwhile recording corrections to (8) and (14) of reference 4.

Equation (8) should read:

$$|p_r'|^2 = \left[\left(\cosh\frac{2(H+J)}{n} - \cos\frac{2r-1}{n}\pi\right) \times \left(\cosh\frac{2(H-J)}{n} - \cos\frac{2r-1}{n}\pi\right)\right]^{1/2} \div \left(\cosh\frac{2H}{n} + \cos\frac{2r-1}{n}\pi\right)$$

Equation (14) should read:

$$\Gamma(p) = \frac{K_o}{(p + p'_{(n+1)/2})}\prod_{r=1}^{(n-1)/2}\frac{(p^2 + |p_r|^2)}{(p^2 + P_r' p + |p_r'|^2)}$$

Neither of the methods described takes into account the exact frequency variation of the coupling susceptances B_i in the actual filter. This variation can cause significant differences between the transformed prototype response and the final filter response, particularly at high values of skirt rejection. It is therefore prudent at this stage to

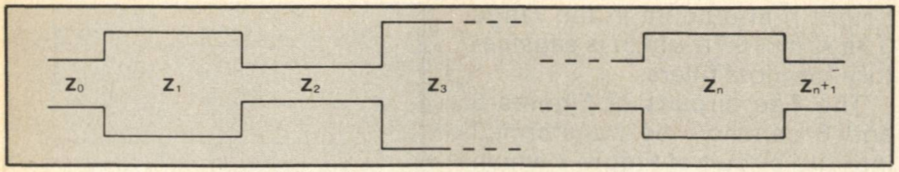

Fig. 4 Distributed low-pass prototype filter.

perform a detailed computer analysis of the filter performance using the actual frequency behavior of the geometry to be used, so that small adjustments can be made if necessary. Phase response and group delay are also calculated at this point if these are pertinent to the filter specification.

Filter Realization

Having derived the required susceptance values B_i and positions θi using one of the methods described, it is necessary to design a structure which will insert these correct values into the waveguide. Rows of inductive posts or irises are generally used and their susceptance values obtained from published data[5,6] or from experimental results. These data are approximate and tend to ignore thickness effects so that many filter designs include adjustable tuning screws for trimming the susceptance of the inductive elements. These techniques though adequate at low frequencies become impractical for millimeter-wavelengths.

The diameter or thickness of the posts or irises has to be made much larger in relation to the waveguide dimensions in order for the structure to be manufactured. The "zero thickness" approximation no longer holds. Furthermore the use of susceptance trimmers, besides being limited by lack of space in the small waveguide sizes, is highly undesirable since they can add markedly to the overall insertion loss of the filter. An accurate estimate of the susceptance of thick inductive obstacles in waveguide is needed.

Figure 5 shows the geometry of a post doublet in waveguide together with its equivalent circuit in the form of a tee network containing shunt and series reactances X_b and X_a, normalized to the characteristic impedance Z_o.

Marcuvitz[5] gives expressions for the shunt and series reactances of a single post offset from the center of the waveguide, and Gruenberg[7] derives the shunt reactance of a post doublet assuming that no series term exists. Combining these results yields the following expressions for the circuit elements X_a and X_b.

$$X_a \simeq \frac{a}{\lambda_g}\left[\left(\frac{1.4a}{\lambda_o}\right)^2 G - F\right] + \frac{1}{2} X_b$$

$$X_b \simeq \frac{a}{\lambda_g}\left(\frac{\pi d}{a}\right)^2 \sin^2 \frac{\pi c}{a}$$

where

$$F = 1 + \frac{1}{4}\operatorname{cosec}^2\left(\frac{\pi c}{a}\right)\left(\ln\frac{\pi d}{4a} + \ln\cot\frac{\pi c}{a}\right)$$

$$\text{and } G = \operatorname{cosec}^2\left(\frac{\pi c}{a}\right)\sum_{\substack{\text{odd } m=3}}^{\infty}\frac{1}{m^2}\left(\frac{\pi d}{2a}+\frac{1}{m}\right)\left(1+\frac{1.5}{m^2}\right)\sin^2\left(\frac{m\pi c}{a}\right)e^{\frac{-m\pi d}{2a}}$$

The infinite series for the term G converges rapidly and for practical purposes can be truncated to 10 terms.

These expressions give excellent results for post diameters up to around .15a provided the posts are not too close to the waveguide wall or to each other.

The assymetric inductive iris is shown in Figure 6 together with its equivalent circuit representation which is similar to that for posts.

Developing the formula given by Marcuvitz[5] for an asymmetric iris of zero thickness, it may be shown that, for iris thickness t, the circuit elements X_a and X_b are well approximated by the following expressions.

$$X_a \simeq \frac{X'(X_b^2+1)}{2X'X_b+1}$$

$$X_b \simeq \tan(k_1 h^2 t + k_2 t)$$

Where X' is the shunt reactance of an equivalent iris of zero thickness and height h'.

X' is given by Marcuvitz.

$$\text{i.e. } X' = \frac{a}{\lambda_g}\frac{\tan^2 \pi\frac{(a-h')}{2a}}{1+\operatorname{cosec}^2\pi\frac{(a-h')}{2a}}\cdots$$

$$\left\{1+\frac{8\alpha^4\beta^2 Q}{1+\alpha^2+\beta^6(\beta^4+6\alpha^2)Q} + 2\left(\frac{a}{\lambda_o}\right)^2\left[1-2\frac{\alpha^2+2\beta^2\ln\beta}{\alpha^4(1+\alpha^2)}-\frac{2\alpha^4\beta^2}{1+\alpha^2}\right]\right\}$$

where

$$h' = \frac{h+k_3 t}{1-k_4 t}$$

$$\alpha = \sin\pi\frac{(a-h')}{2a} \qquad \beta = \cos\pi\frac{(a-h')}{2a}$$

$$\text{and } Q = \left[1-\left(\frac{a}{\lambda_o}\right)^2\right]^{-\frac{1}{2}} - 1$$

The K's which are empirically derived constants are given to 4 decimal places as:

$k_1 = .0017$ $k_2 = .0713$
$k_3 = .3361$ $k_4 = .0209$

These expressions work well for iris thickness t up to around .15a provided the iris is not too low or too high. As a guide, the iris

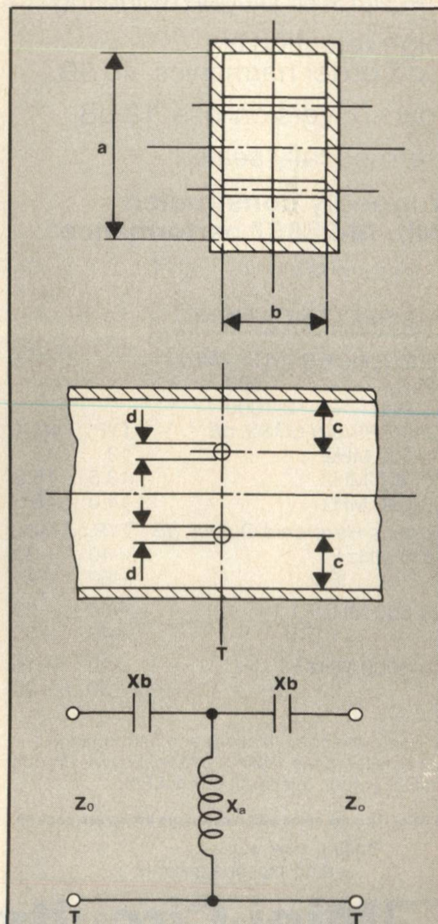

Fig. 5 Geometry and equivalent circuit for post doublet in waveguide.

[Continued on page 94]

[*From page 93*] **FILTERS**

height h should lie in the range 0.3a < h < 0.7a which is satisfactory for most filters.

The Tee circuits of Figures 5 and 6 can now be transformed into the circuit of Figure 7 which contains pure shunt susceptance at terminal planes T′ located a distance x at either side of terminal plane T.

The susceptance B and the terminal plane shift x are expressed in terms of the reactances of Figs 5 and 6 by the equations:

$$B = \frac{2X_aX_b - X_b^2 - 1}{X_a}$$

$$x = \frac{\lambda_g}{2\pi} \tan^{-1} X_b$$

It is now a simple matter to choose the post or iris dimensions so that the normalized susceptances B of Figure 7 match the B_i/Yo required by the filter theory. At the same time, the section lengths θ_i are corrected by the terminal plane shifts x_i associated with each iris or post doublet. This technique works extremely

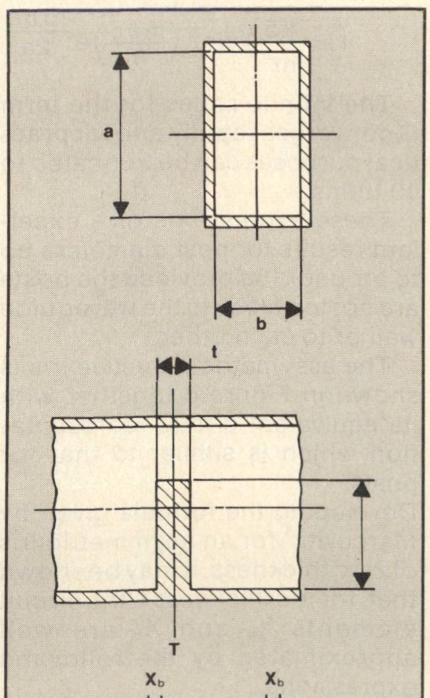

Fig. 6 Geometry and equivalent circuit for assymetric iris in waveguide.

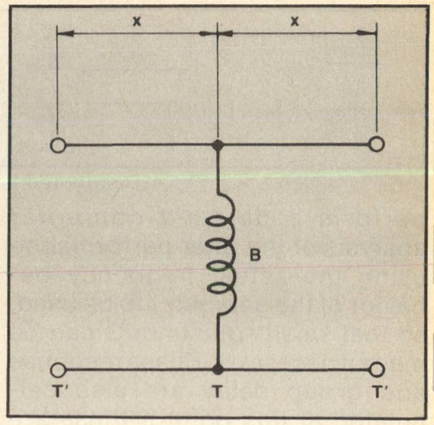

Fig. 7 Transformed equivalent circuit.

well within the limits of validity indicated, giving remarkably accurate agreement between computer predicted responses and measurement on real filters. The ability to estimate accurately the behavior of waveguide obstacles of appreciable thickness leads to a practical system of construction for millimeter-wave filters.

Filter Construction

Inductive posts can be used successfully up to around 40 GHz, but the difficulties of accurate location in the waveguide preclude their use at higher frequencies. Irises on the other hand, provided they are thick enough to be mechanically stable, can be made an integral part of the waveguide assembly. Filter bodies are N C machined from solid high-conductivity copper with a separate flat lid soldered in position by a carefully controlled oven technique. The construction is illustrated in Figure 8.

Tolerance analysis has shown that a machining accuracy of around 5 microns is required for repeatable performance at 140 GHz, and this is within the capabilities of modern precision machines. Even with such close tolerances, however, it is necessary to include adjustment for fine tuning of the filter cavities. Tuning slugs constructed from a low-loss dielectric such as quartz or sapphire are used in place of conventional metallic screws which tend to be lossy and unreliable at millimeter-wave frequencies. The slugs are mounted midway between each iris along the waveguide center-line, each filter section being shortened by a small amount so that fine tuning is

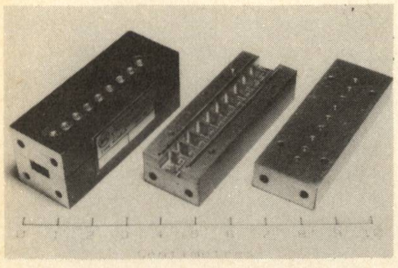

Fig. 8 Nine-section Ka-band filter.

accomplished with minimal slug insertion.

Experimental Results

Figure 9 shows the predicted and measured results for the 9-section Ka-band filter illustrated. The measured responses show excellent agreement with the computer predictions, and the measured insertion loss is very low at around 0.5 dB over most of the band. This filter is now in full production.

Conclusion

A workable technique for the design, realization and production of millimeter-wave direct-coupled waveguide filters has been developed. The methods employed are directly appliable up to around 140 GHz offering the millimeter-wave systems designer a high performance alternative to filters constructed in other transmission line media.

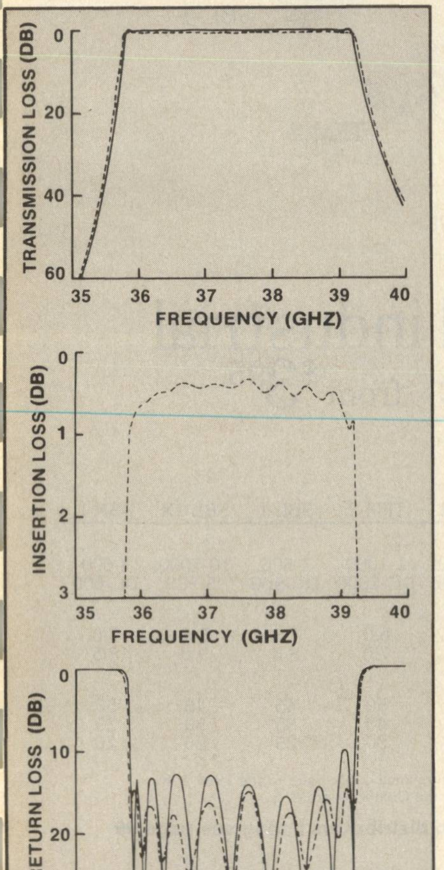

Fig. 9 Computed and measured results for 9- section Ka-band filter.

Acknowledgements

The author wishes to thank the directors of MM Microwave Ltd. for permission to publish this work, and Dr. M. J. Howes for his help in the preparation of the manuscript.

REFERENCES

1. Cohn, S. B. "Direct-Coupled-Filters" Proc I.R.E., Vol. 45, February 1957
2. Matthaei, Young, Jones, *"Microwave Filters, Impedance-Matching Networks and Coupling Structures".* New York: McGraw-Hill
3. Levy, R. "Theory of Direct-Coupled Cavity Filters" IEEE Trans MTT-15, June 1967
4. Levy, R., "Tables of Element Values for the Distributed Low-Pass prototype Filter." IEEE Trans MTT-13, September 1965
5. Marcuvitz, N., *"Waveguide Handbook"*, McGraw Hill
6. *Microwave Engineer's Handbook"* *Artech House Inc., Dedham, MA. May 1982
7. Gruenberg, H., "Symmetrically Placed Inductive Posts in Rectangular Waveguide." Canadian Journal of Physics, Vol 30, 1952

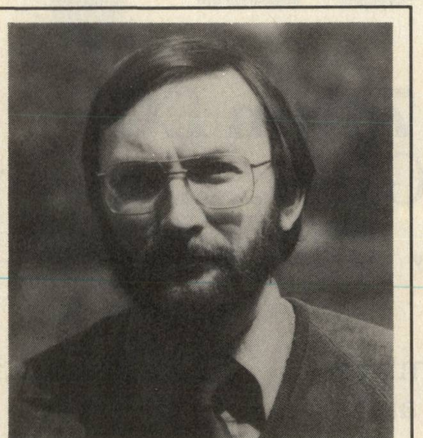

John Bratherton, *received his B.Sc. degree in mathematics and physics from King's College, University of London in 1970. In the same year he joined Plessey Radar Ltd., Isle of Wight, where he worked on the design and development of radar antennas and radomes, specializing in frequency-scanning array antennas. In 1979 he joined MM Microwave Ltd as Senior Microwave Engineer where he has been involved in a wide range of component design projects. He is keenly interested in the application of computer aided microwave circuit modelling to component design, and is presently engaged in the development of filters, millimeter-wave components, and microwave subsystems.*

■

A SAW Analog Correlator Using the Chirp Transform

V.H. Estrick and G.W. Judd
Hughes Aircraft Company
Fullerton, CA

Introduction

Modern radar and communications systems often employ waveforms significantly more complex than the simple modulation schemes used in the past. This increased complexity results from the need to operate in dense dynamic signal environments which include both friendly interference and intentional jamming. The radar case includes the need to separate and identify targets embedded in large clutter. To efficiently cope with such environments, these systems are often equipped with variable waveforms which allow modification of bandwidth, pulse length, modulation format, etc., depending on a specific situation.

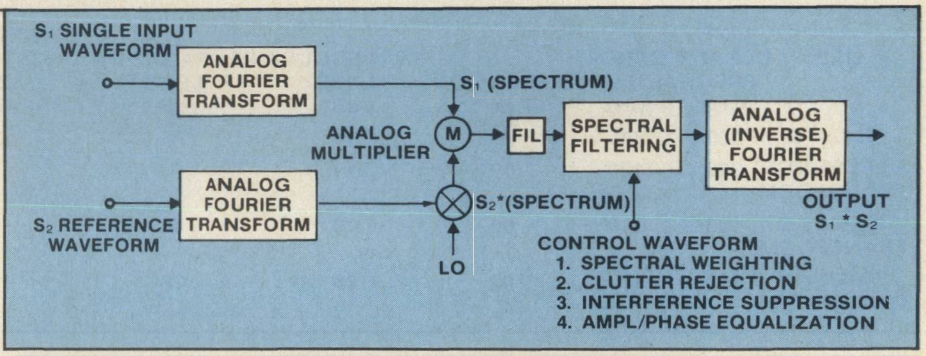

Fig. 1 Block diagram of a programmable correlator using Fourier transforms.

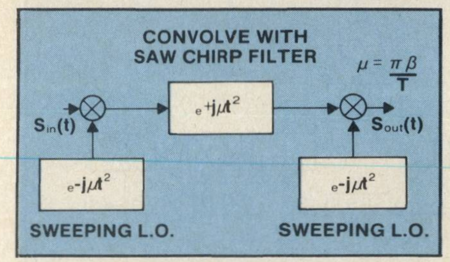

Fig. 2 Multiply-convole-multiply implementation of chirp transform algorithm.

TABLE I

ACTC CHARACTERISTICS AND PERFORMANCE GOALS

PARAMETER	GOAL
Input Signal Bandwidth (Max.):	60 MHz
Input Signal Duration (Max.):	30 μSEC
Dynamic Range:	$\geq$50 dB
Input Power Levels:	-30 dBM TO +10 dBM
Supression of Spurious Signals:	$\geq$30 dB
Primary Power Input to CTC:	1100 VAC
SAW Substrate Material:	$LiNbO_3$

These system concepts and requirements result in a recognized need for programmable signal processors. Such processors, upon command will provide the "matched filter" to the selected waveform, maximizing the signal-to-noise ratio.

Two programmable analog signal processors have been developed utilizing the chirp transform algorithm to perform the Fourier transform operation [1]. The first processor, called the Chirp Transform Correlator (CTC) and developed under ERADCOM contract DAAB07-76-C-1298, proved the concept of the processor architecture [2]. The second, more advanced processor called the Asynchronous Chirp Transform Correlator (ACTC) was developed under ERADCOM contract DAAB07-78-G004 [3]. The configuration of a chirp transform signal processor implemented in the form of a correlator is shown in Figure 1. This configuration makes use of the fact that the correlation of two signals is equivalent to the inverse Fourier transform of the product of the first signal Fourier transform and the complex conjugate of the second signal Fourier transform [1]. As shown in Figure 1, stored reference waveform S2 and a signal S1 are fed into the CTC where, for a radar application, S2 would be the transmitter drive signal and S1 the radar return. For analog processors the output of the signal and reference transform are waveforms which represent the Fourier transform of the two input signals. The reference transform spectrum is inverted, using a fixed local oscillator and selecting the difference frequency out of the mixer. This produces the complex conjugate of the reference waveform required for the correlation process. The resulting waveforms are then multiplied together and passed through an inverse transform operation, giving an output that represents the cross correlation of S1 and S2. If S1 and S2 are the same, the output is the auto-correlation or matched filter response of the signal.

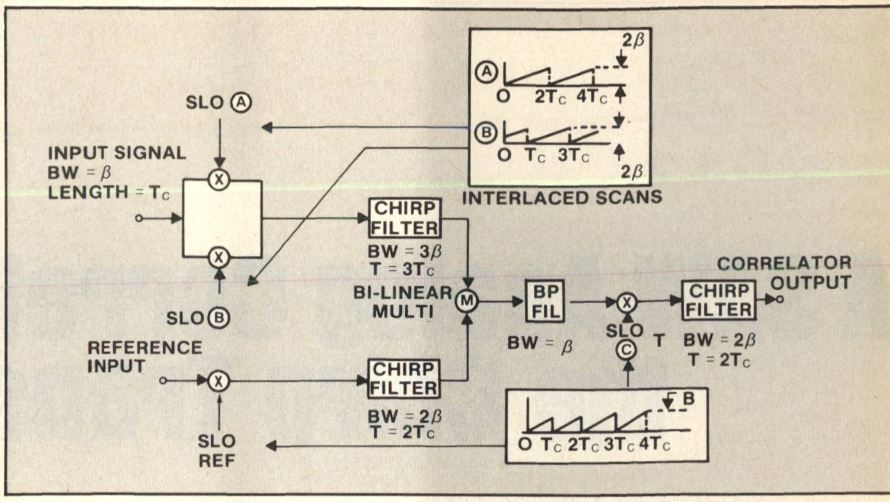

Fig. 3 Block diagram of the asynchrononous chirp transform correlator. The interleaving of the sweeping LO's provides 100% probability of encompassing input pulses.

TABLE II

SUMMARY OF RAC MIDBAND LOSS DESIGN PARAMETERS

USE	LINE CENTER FREQ MHz	BAND-WIDTH MHz	DISPERSION µs	TRANSDUCER LOSS dB	PROPAGATION LOSS dB	NON-SYNCHRONOUS SCATTERING LOSS dB	REFLEC-TION LOSS dB	OVERALL DESIGN LOSS dB	MEASURED LOSS dB
SLOA, B	200	60	60	18	7.5	2.5	8	36	37
REFERENCE TRANSFORM	300	120	60	19	8	2	16	45	47
INVERSE TRANSFORM	400	120	60	20	8	2	21	55	58
SIGNAL TRANSFORM	400	180	90	20	12	2	21	55	64

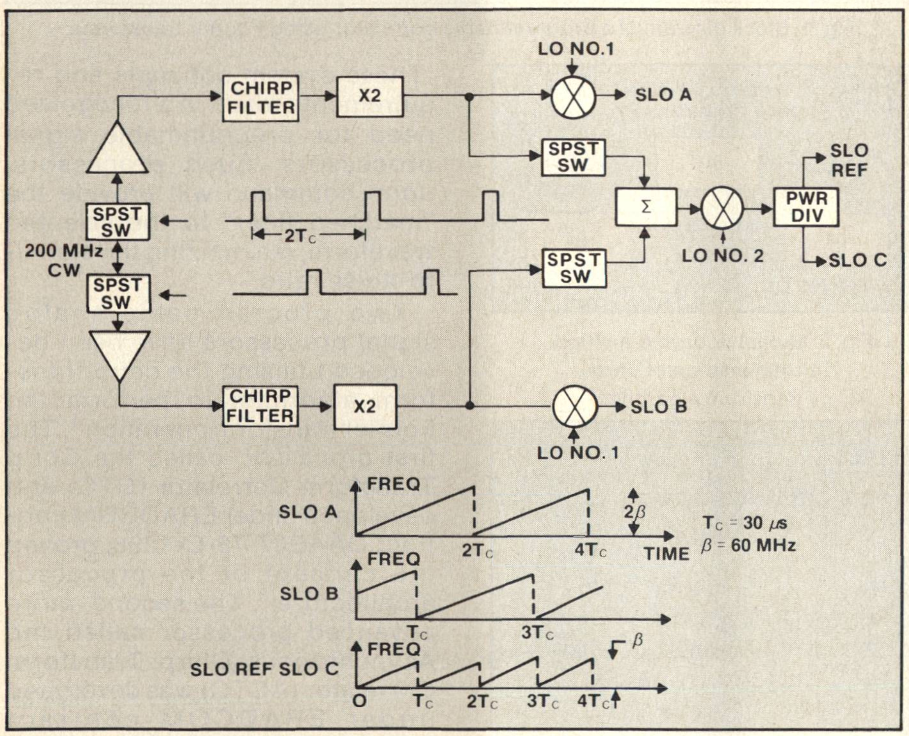

Fig. 4 Block diagram of the sweeping local oscillator (SLO) generator used in the ACTC showing the location of the X2 multipliers which double the frequency deviation of signal out of the chirp filters.

The Chirp Transform Algorithm

The Fourier transformation of the signals can be obtained by using the chirp transform algorithm shown in Figure 2. The three operations required to implement the algorithm are:

- multiplication of the imput signal by a linearly sweeping local oscillator (SLO),
- convolution of the resulting signal through a linear FM dis-

[Continued on page 100]

[*From page 98*] **CORRELATOR**

persive filter (chirp filter), and
- a final multiplication with an SLO.

The frequency versus time slopes of the SLOs are opposite that of the chirp filter. This is the multiply-convolve-multiply form of the chirp transform, but a convolve-multiply-convolve form of the algorithm also exists [1]. In practice, the linear FM SLOs and the convolution chirp filter can be constructed using linear FM surface acoustic wave (SAW) dispersive delay lines.

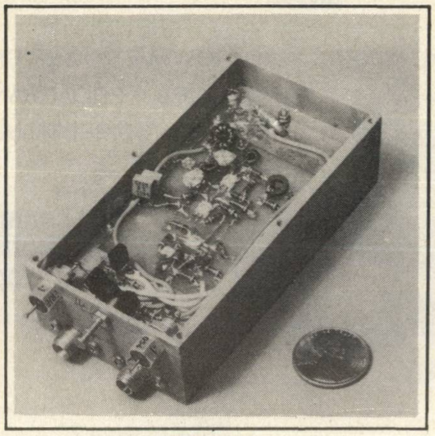

Fig. 5 Bilinear multiplier.

Asynchronous Chirp Transform Correlator

The Chirp Transform Correlator (CTC) developed under the first program proved the basic operation of the concept for a variety of flat spectrum input waveforms such as linear FM. However, its configuration was designed such that input signals and the SLOs were required to be time conincident to obtain complete correlation. However, many signals of interest do not cooperate and are received at arbitrary times. For this a more general processor is required, one which can operate asynchronously. This requirement led to the development of the Asynchronous Chirp Transform Correlator (ACTC) [3].

The objectives of the ACTC development task were to design, fabricate, test, and demonstrate a more advanced version of the chirp transform signal processor developed previously. The ACTC added asynchronous operation which allows correlation of incoming signals independent of their time of arrival. It also cross-correlates signals having nonuniform spectra, such as a nonlinear FM, PSK, and gated CW waveforms, and provides for CW interference rejection. The performance goals and actual performance comparisons for the ACTC are listed in Table 1, and a simplified block diagram provided in Figure 3. asynchronous operation which tained by using two SLO chirps (A and B), each of duration $2T_c$, which are independently mixed with the input signal. The two chirps are interleaved so that an input signal of duration up to T_c will always fall completely within at least one chirp time interval. Thus, the accurate Fourier transform of the input signal is generated by the processor independent of its time of arrival with respect to the SLO chirps. A transformed input signal and transformed reference signal produce time coincident CW tones (with an amplitude modulation that is a function of the input waveform) whenever the input signal and reference are

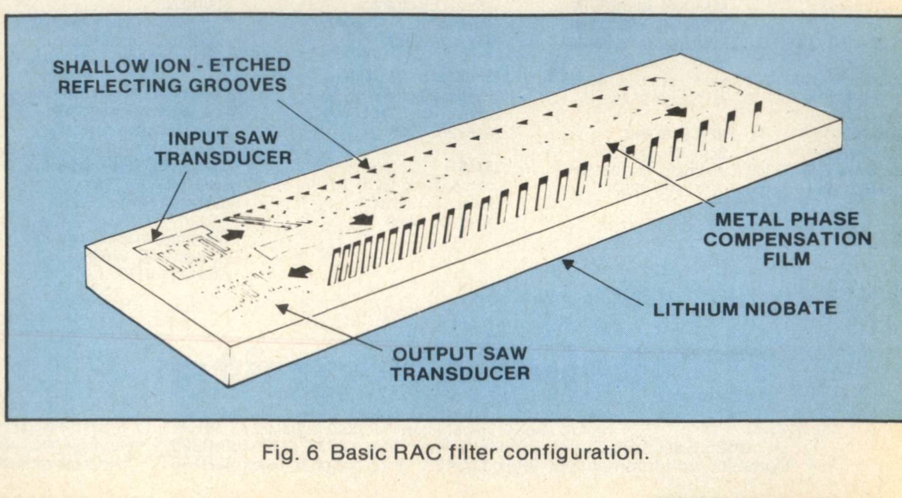

Fig. 6 Basic RAC filter configuration.

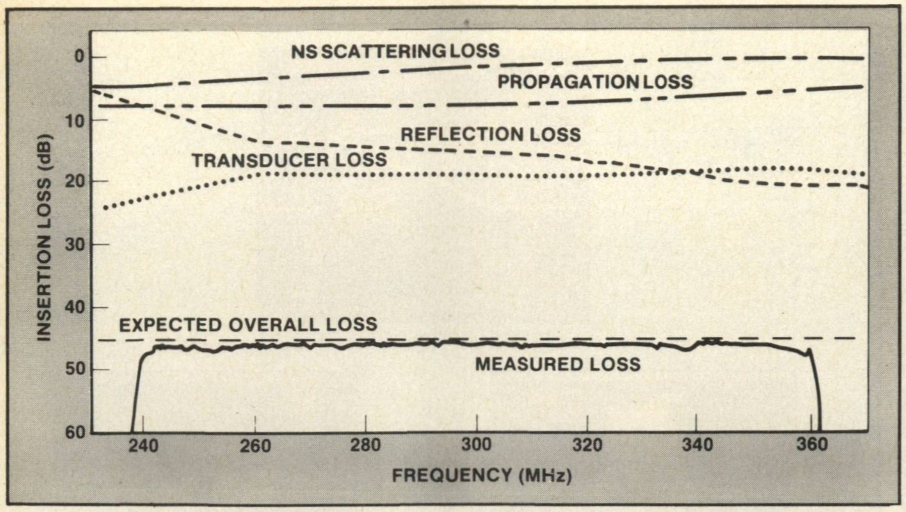

Fig. 7 Loss curves used in the design of the 120 MHz by 60 us RAC line. The measured midband loss of the delay line was within 2 dB of its 45 Db design value.

identical. The exact frequency of the multiplier output is directly proportional to the time of arrival of the signal relative to the reference waveform. Thus, the frequency of the multiplier output signal can be used as a measure of target range if the ACTC is used to process a radar return. This technique is similar to those used in FM/CW radars to measure range. The final transform stages convert this signal to the desired correlated pulse output. The bandpass filter following the multiplier is designed to pass only one frequency band, namely the one that is derived from the accurate input signal transform and reject those produced from the opposite SLO.

For input signals with B = 60 MHz and T_c = 30μs SLO A and SLO B signals are required to sweep 120 MHz in 60μs while SLO ref and SLO C sweep 60 MHz in 30μs. Likewise, the chirp filter in the signal path has a bandwidth of 180 MHz, while the RAC filters in the reference path and at the output have 120 MHz bandwidths. The slopes of the transform RAC filters and the SLOs are identical at 2 MHz per microsecond.

The SLO chirp waveforms (SLO A, SLO B, SLO ref and SLO C) are produced by the sweeping local oscillator generator shown in Figure 4. Two interleaved chirps are generated by alternate impulse excitation of the two identical chirp filters, and a frequency doubler is used to obtain twice the frequency excursion available directly from the chirp filters. Following the doubling, mixing with a fixed local oscillator produces the SLO A and SLO B waveforms at the desired center frequency. The SLO reference and SLO C waveforms are obtained by simply gating the A and B waveforms and mixing the resultant output to a different center frequency.

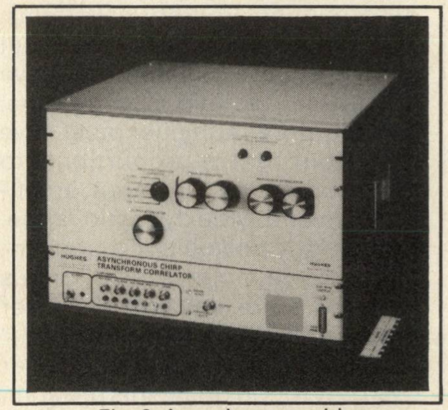

Fig. 8 Asynchonous chirp transform correlator.

The decision to use frequency doubling rather than direct generation of the 120 MHz bandwidth waveforms was based on considerations of waveform accuracy and signal-to-noise ratio requirements of the SLO chirp signals. It was determined that phase errors in a 60 MHz bandwidth chirp filter would be significantly less than half those of the 120 MHz filter. Thus, lower errors would result after doubling. Also, the narrowband filter has at least 3 dB lower insertion loss, and can withstand about 6 dB greater drive power than a 120 MHz bandwidth filter, thereby allowing a better signal-to-noise ratio on the SLOs.

[Continued on page 102]

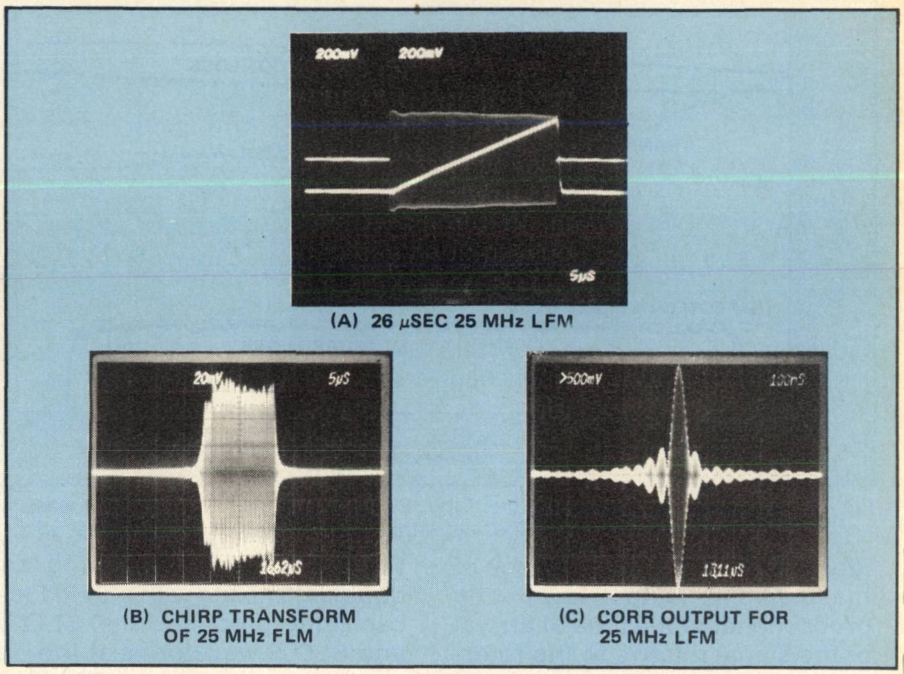

(A) 26 μSEC 25 MHz LFM

(B) CHIRP TRANSFORM OF 25 MHz FLM

(C) CORR OUTPUT FOR 25 MHz LFM

Fig. 9 Autocorrelation of 26 μs by 25 MHz linear FM pulse using the ACTC.

Bilinear Multiplier

A key component in the ACTC design is the bilinear multiplier circuit in providing the versatility of correlating arbitrary waveforms, since the transforms of the input and reference signals may have amplitude variations with time. The required multiplier must have an output that is proportional to the product of the input amplitudes over a wide dynamic range. This is not possible if a conventional diode mixer is used for this function, since one port of a mixer must be driven into saturation.

A specialized bilinear multiplier was developed under this program using a four-quadrant Gilbert transconductance multiplier[4]. The multiplier, fed with two imputs, X and Y, produces an (X times Y) output. For the ACTC application, the Y-input operates over a frequency range from 240 to 360 MHz and the X input from 310 to 490 MHz. The output is tuned to the difference frequency (centered at 100 MHz) of the two inputs. The multiplier shown in Figure 6 was constructed using matched pair NEC transistors (NE32740As) and otherwide discrete components.

SAW RAC Filter Characteristics

Of the many techniques that have been developed for implementing SAW chirp filters, the reflective array compressor (RAC) design approach[5] is ideally suited for producing the precise linear FM dispersion characteristics with large time-bandwidths required for the ACTC. The key elements of a typical RAC filter are shown in Figure 6. The linear FM dispersive delay characteristics of the RAC filter are determined by the spacing and depth of reflecting grooves that are ion-beam etched into the crystal substrate. The surface wave generated by the input transducer travels along the reflective gratings until it reaches the point where the spacing of the grooves matches the acoustic wavelength. At this point, a portion of the wave is reflected by the slanted grooves to the second grating. The opposite slope grooves in the second grating reflect the wave back to the output transducer, where it is converted back to an RF output signal. The groove spacings are accurately varied along the length of the gratings to produce a precise linear change in the reflection path as a function of frequency. Since the RAC filter characteristics are determined by mechanical-type reflections from the etched grooves rather than by the electro-acoustic interactions used in conventional despersive transducers, they exhibit considerably lower distortion effects as compared to the levels found in SAW chirp filters made with long interdigital transducers. RAC filters are essentially unaffected by spot defects in the reflecting arrays, and thus are much more tolerant to typical processing errors that lead to severe transducer defects in conventional SAW devices. The RAC's amplitude response is controlled by varying the depth of the reflecting grooves. Thus, by tailoring the groove profile, it is possible to compensate for various loss effects, thereby producing a flat amplitude response over the operating bandwidth of the filter. Since the propagation path of the acoustic signal in a RAC line is folded, the RAC filter can achieve twice the dispersive time delay available in a conventional SAW filter for a given crystal length.

Another important feature of RAC devices is that their phase errors can be compensated with the simple addition of a variable-width metal film between the two reflecting arrays. This slows down the surface wave and adds a phase delay, depending on the film width. These films can be individually tailored to compensate for the measured errors in a particluar filter, and can reduce the delay errors in a line to a few parts per million. The tight control of the frequency versus time characteristics and the inherent low phase errors of RAC devices is largely responsible for the successful application of chirp transform processing techniques in current wideband processing networks [6, 7]

RAC Design and Performance Characteristics

The RAC devices used in the ACTC follow the design procedures developed by Gerard and Otto where the relative reflection loss of the gratings is varied to compensate for the amplitude response variations of the input transducer and major propagation loss effects to produce a flat overall filter response [8]. Figure 7 shows each of the loss factors that, when added together, produce the overall response of the 120 MHz by 60μs RAC filter used in the reference transform. As shown in the figure, the measured response of this delay line was within 2 dB of the 45 dB design value over the full 120 MHz operating bandwidth. Principal design values used for the filters in the system are listed in Table II.

The measured insertion loss of the RAC filters was within 3 dB of the design value for all but the 180 MHz by 90μs device. The measured response of this line was found to roll off quite rapidly to a midband loss value of 64 dB, and

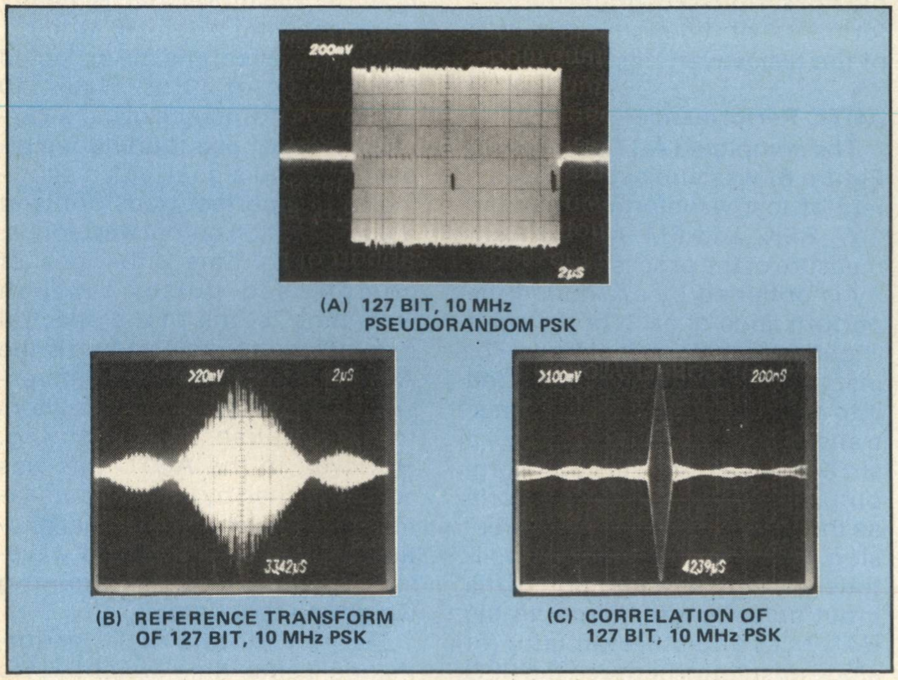

(A) 127 BIT, 10 MHz PSEUDORANDOM PSK

(B) REFERENCE TRANSFORM OF 127 BIT, 10 MHz PSK

(C) CORRELATION OF 127 BIT, 10 MHz PSK

Fig. 10 Autocorrelation of 127 bit 10 MHz PSK waveform using the ACTC.

[Continued on page 104]

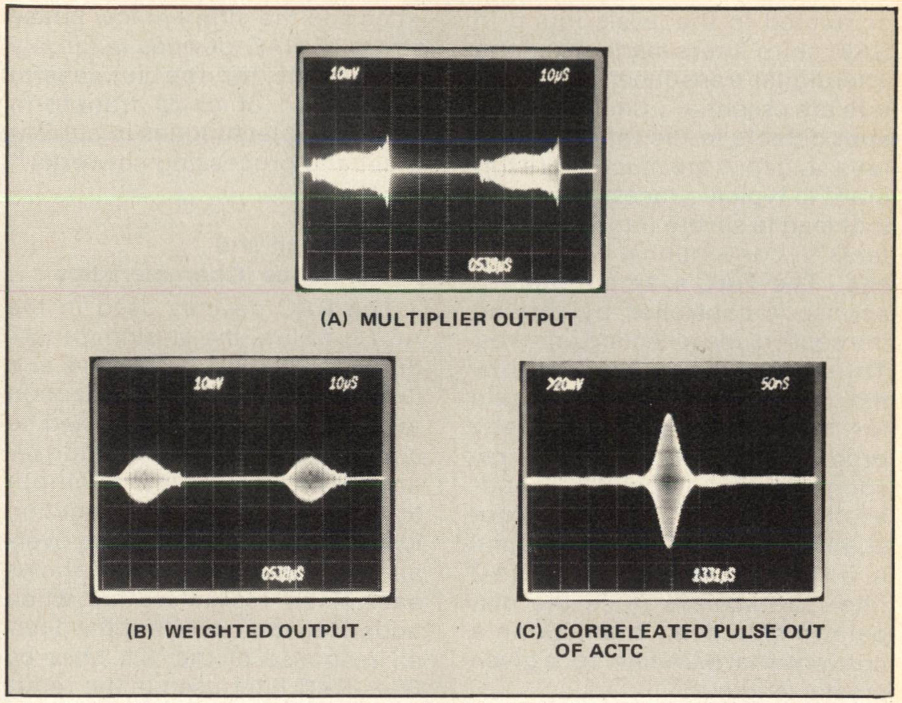

(A) MULTIPLIER OUTPUT

(B) WEIGHTED OUTPUT

(C) CORRELEATED PULSE OUT OF ACTC

Fig. 11 ACTC performance for a 12 μs, 60 MHz chirped input using time weighting to reduce sidelobes.

exhibited unusually high loss variations of more than 10 dB. The 16000 time-bandwidth product of this filter represents the current state of the art in RAC filter design, and is not easy to fabricate. However, previous devices made with these waveform parameters were found to have reasonably flat amplitude responses and had insertion losses of only 57 dB. Fortunately, the excess loss and amplitude variations of this line did not seriously degrade the performance of the system for most of the test waveforms.

ACTC Performance

The completed ACTC (shown in Figure 8) was subjected to a variety of test waveforms including CW, PSK, and FM. A significant measure of the processor capability is obtained by examining the performance of each of the chirp (Fourier) transform functions. For instance, a pulsed CW signal fed into either the signal or reference transform path input produces a sin X/X waveform at the transform output which is of the same form as the output of a pulse compression line. The transform amplitude will vary as a function of the input pulse length. Errors in the RAC lines and other circuitry (or slope mismatch between the SLO and convolution RAC lines) result in an amplitude loss and output pulse broadening.

The correlation properties of the ACTC were evaluated using a variety of waveforms, including gated SW, PSK and both linear and nonlinear FM. Figure 9 shows the performance using a VCO-generated 25 MHz by 25μs FM chirp test signal. The chirp transform (B) of this waveform shows a slight asymmetry caused by VCO nonlinearities, but the auto-correlation waveform (C) is nearly ideal, showing sidelobes within 1 dB of theoretical and the expected pulse width of 40 ns. Figure 10 depicts performance using a 127-bit, 10 MHz pseudorandom biphase coded signal, again showing nearly perfect transform and autocorrelation output waveforms.

Reducing time sidelobes of compressed pulses through weighting is one of the spectral manipulations implemented in the ACTC. Traditional pulse compression systems use bandpass filters to accomplish the weighting. However, in the ACTC this was accomplished by using a modulator placed behind the bilinear multiplier driven by a shaped waveform simulating a Hamming weighting function.

Figure 11 shows ACTC performance using time weighting to reduce sidelobes. The bilinear

[Continued on page 106]

[From page 104] **CORRELATOR**

multiplier output using a 12μs 60 MHz as a test signal is shown in detail (A). The output of the modulator (B) after application of the weighting is also shown along with the resultant compressed pulse (C) with a peak sidelobe level of 26 dB. The advantage of this technique is that filtering can be accomplished using time modulation, allowing in addition to time side lobe weighting, CW rejection technique techniques.

Future Applications

The major advantage of the CTCs are their large time-bandwidth product and adaptability for any waveform within the processor's time and bandwidth windows. Even with advances in high-speed digital technology, the CTC can provide superior performance for wideband short duration waveforms. In addition, the CTC technology provides low-power, real-time signal processing which is available today and does not require years of development. Also, attractive applications combining analog chirp transforms and digital processing have been developed, where digital signals have been up-converted to CTC frequencies, processed, and then converted back to digital [6, 7].

The ACTC unit weighs 51 pounds and occupies a volume of 2.5 cubic feet. The power consumption is about 260W with 150W required for the RAC ovens. Future processors could certainly be made smaller than the demonstration model ACTC reported here. Interestingly, the ACTC is about two-thirds the volume of the original CTC despite the additional capability. Only minor attention was given to size, and it is estimated future processors could benefit from a significant size reduction, to less than 1/2 cubic foot, through improved packaging.

Acknowledgements

The authors would like to thank Mr. S. Schenk for his development of the bilinear multiplier circuit and Mr. G. P. Jones and Mr. J. Perkins for their dedicated effort to design, fabricate and test the ACTC.

Special thanks are due to Mr. W. Skudera and Mr. E. Mariani of the US Army ERADCOM for their support of this program.

Vaughn H. Estrick, *a Senior Staff Engineer in the Adaptive Techniques Department at Hughes Ground Systems Group in Fullerton, California, was the Technical Director and Project Manager of the U.S. Army ERADCOM SAW Programmable Matched Filter Project, which included the Asynchronous Chirp Transform Correlator. Previously Section Head of the Receiver/Exciter Section, he was responsible for the RF and IF hardware in the Hughes ground based radars, including AN/TPQ-36 and AN/TPQ-37 Firefinder, AN/SPS-52, and the improved Point Defense Target Acquisition System (IPD/-TAS. Mr. Estrick received his BS in Electrical Engineering at the University of Idaho, Moscow, Idaho in 1962, and his MS in Electrical Engineering at the University of Southern California in 1964.*

Gordon W. Judd, *is head of the Acoustic and Optical Techniques Section in the Radar and Communication Division of Hughes Ground Systems Group. He has worked on the development of SAW devices since 1969 and is currently involved with the application of large time bandwidth chirp filters in analog signal processing systems. Mr. Judd received his BSEE degree from the University of Idaho in 1966 and a MSEE degree from the University of Southern California in 1969.*

REFERENCES

1. Gerard, H.M. and O.W. Otto, "Performance of a Programmable Radar Pulse Compression Filter Based on Chirp Transformation with RAC Filters," 1977 IEEE Ultrasonics Symposium Proceedings, pp. 947-951.
2. Gerard, H. M. and O. W. Otto, "Surface Wave Chirp Transform Correlator — Final Report (Phase Two)," Report No. DELET-TR-76-1298-F2, U.S. Army ERADCOM, Fort Monmonth, N.J. (1978).
3. Bristol, T.W., et. al., "SAW Programmable Matched Filters-Interim Report," Report No. DELET-TR-78-3004-1, U.S. Army Electronics Research and Development Command, Fort Monmonth, N.J. (1980).
4. Gilbert, B., "A Precise Four-Quadrant Multiplier with Sub-Nanosecond Response," IEEE Trans Solid State Circuits, Vol. SC-3, pp. 365-373, Dec. 1968.
5. Williamson, R.C. and H.I. Smith, "The Use of Surface-Elastic-Wave Reflection Gratings in Large Time-Bandwidth Pulse Compression Filters," IEE Trans. MTT-21, pp. 195-206, April 1973.
6. Willilamson, R.C., "Wideband SAW Fourier-Transform Processor Design and Applications," IEE Conf. Publ. No. 180, pp. 237-242, Dept. 1979.
7. Gautier, H. and P. Tournois, "Signal Processing Using SAW and Digital Components," Proc. IEE on Comm. Radar Signal Processing, April 1980.
8. Gerard, H.M. and O.W. Otto, "Development of a Broadband Reflective Array 10,000:1 Pulse Compression Filter," 1974 IEEE Ultrasonics Symp. Proc., IEEE Cat. No. 74CHO-896-ISU, pp. 197-201, Oct. 1973. ■